Materials Systems Inc.

Near Net-shape Fabrication of Ultrafine Scale Piezoelectric Ceramic/Polymer Composites

Final Report: November 1997

Contract Number N00014-92-C-0212

Submitted to:
Office of Naval Research
Arlington, Virginia

in fulfillment of contract requirements

Contractor:
Materials Systems Inc.
521 Great Road
Littleton, MA 01460

Executive Summary

In this program, new net-shape forming technologies were developed for producing fine scale 1-3 and 2-2 piezoelectric ceramic/polymer composites. Piezocomposite materials having extremely fine piezoceramic elements were fabricated using a modified ceramic injection molding process similar to that developed by MSI [1] for coarse scale piezocomposite manufacturing. The principal technical challenges were to make extremely fine PZT ceramic 1-3 and 2-2 preforms without defects or distortion, and use these to and produce piezocomposite samples having sufficient thickness to achieve lateral mode-free response. PZT rods and strips having width dimensions in the order of 25 to 600 μm and length-to-width aspect ratios in excess of ten were demonstrated on a research scale. These were used for experimental demonstration of high frequency acoustic imaging arrays for medical ultrasound and Navy mine hunting applications.

The new piezocomposite fabrication technology is finding applications ranging from diver-held sonar to low frequency mine detection and classification to advanced net-shape piezoelectric actuators. The program has influenced development of net-shape formed accelerometers for active surface control, as well as coarse receive arrays for submarine use. Under separate SBIR funding (ONR Contract number N00014-95-C-0117), the fine scale molding technology has been scaled up to the point where large (150 x 50 mm) pieces having pitch dimensions below 200 μm can be produced every few minutes.

Prior to this work, the only net-shape forming approach available for producing piezocomposite was one developed by Siemens [2] which utilized ceramic slip casting into fugitive molds produced by x-ray photolithography. The new fine scale ceramic injection molding approach developed by MSI has allowed molds to be re-used time and again for manufacturing net shape 1-3 and 2-2 piezoelectric ceramic/polymer composites, offering significant cost savings over conventional dice-and-fill techniques and the fugitive mold approach. This process has made possible the construction of composite transducers having more complex ceramic element geometries than those previously available, allowing greater design flexibility for improved acoustic impedance matching, lateral mode cancellation, and superior actuator performance.

Over the course of this program, MSI has shown injection molding technology to be capable of forming 1-3 and 2-2 transducer preforms on an extremely fine scale (1-3 structures with <100 μm wide PZT elements and 2-2 structures with pitches <50 μm). The process has been used to form finished 1-3 composite transducers having element diameters below 150 μm, and 2-2 composites with features less than 25 μm. MSI has continued refining the process and tooling to achieve larger area 1-3 composites, up to 30 mm square with high PZT volume fraction (~60-80%). Throughout the program, MSI has pursued commercialization of these materials, supplying test prototypes under customer funding to both private-sector and Navy composite end-users. As a result, the electro-acoustic properties of these fine-scale composites have been characterized not only by MSI, but also by customers in proprietary applications. In collaboration with Tetrad Corporation, a subcontractor under this program, MSI has verified the performance of these transducer materials through imaging demonstrations on medical ultrasound phantoms at megahertz frequencies.

In addition to ultrafine scale composite synthesis, a major new initiative began in March 1994 into fine scale piezocomposite transducer fabrication for undersea acoustic imaging. The applications drivers were Navy mine hunting systems and diver-held sonar. This task was undertaken as part of a Technical Cooperation Program (TTCP) in conjunction with other organizations in Canada, the UK, and the USA. In particular, MSI worked with a subcontractor, Ultrex (formerly UltraSound Solutions), to demonstrate composite materials configurations that could be used for electronically beam-steered undersea acoustic imaging. A

first generation transducer was designed by Ultrex, built by MSI, and tested by UDI-Fugro in a developmental imaging system. One unanticipated outcome of these tests was the observation of unusual phase and amplitude uniformity in the net-shape formed array elements, which was attributed to tight control of the ceramic firing conditions and the PZT chemistry. The impact of improved array element uniformity was to dramatically reduce the beamforming computation requirements and thus reduce signal processing cost and complexity.

As the program progressed, two net-shape applications tasks were added. The first was to exploit low cost injection molding of velocity sensors for potential use in the CAVES (Conformal Acoustic VElocity Sonar) program. For the second, two, 40 element, 1-3 hydrophone arrays for surface ship mine detection applications were fabricated and delivered to NUWC for testing.

Overall, the program goals were met on schedule and within budget. The program impact was extended beyond fine scale 1-3 and 2-2 piezoceramic molding to include piezocomposite materials evaluation and transducer fabrication demonstrations. A direct link was established between ceramic processing, system cost and imaging performance that would not have been possible without full integration of the materials, transducer design and systems functions under this program. Other defense and commercial arenas can benefit from the availability of fine scale piezocomposite materials. Feedback on applications from Navy and commercial systems end-users has prompted MSI to perform additional exploratory demonstrations of its process for transducers that operate in the 1 to 5 MHz frequency range for therapeutic ultrasound, nondestructive evaluation, and medical imaging.

1. Objective and Deliverables

The program was divided into two major areas:

1) Fine scale piezocomposite synthesis
2) Piezocomposite evaluation.

Other applications demonstrations were:

3) Low Cost Accelerometer Panels
4) Hydrophone Arrays

Fine Scale Piezocomposite Synthesis

The primary objective was to advance the state-of-the-art in near-net shape fabrication of ultrafine scale PZT ceramic/polymer composites. The work was aimed at 2-2 type composites having PZT element dimensions down to 10 μm. For 1-3 composites the ultimate dimensional goal was 25 μm rod diameter. Piezocomposite process scale-up to produce composite pieces 30-50 mm square was another program objective.

In pursuing these objectives, MSI focused on forming processes that were expected to be capable, after scale-up, of economically manufacturing ultrafine scale piezoelectric composites for both Navy and commercial applications.

Piezocomposite Evaluation

This activity was aimed at evaluating the fine scale piezocomposite transducer materials for several Navy applications, including building and testing 1-3 and 2-2 transducer materials and arrays. The latter efforts were accomplished in conjunction with acoustic systems partners, including MSI's TTCP partners and a subcontractor, Tetrad Corporation. The objectives were as follows:

Hydrophones: To collaborate with TTCP partners to better understand, through modeling, transducer fabrication, and testing, how 1-3 piezocomposites improve the performance of hydrophones for flank arrays and other underwater applications.

Multilayer 1-3 transducers: In collaboration with TTCP partners, to develop techniques for fabricating double layer and multilayer 1-3 composite transducers for undersea sensing and actuation.

Piezocomposites for Undersea Imaging: To demonstrate a prototype electronically beam-steered piezocomposite array for use in mine hunting (TTCP) and to demonstrate that net-shape formed piezocomposites can be successfully utilized in high frequency imaging (with Tetrad).

The primary role performed by MSI was to provide composite transducer materials and devices, and to develop techniques for fabricating new piezocomposite transducer configurations for evaluation within the TTCP and by Tetrad. MSI also fabricated several prototype receive arrays which were tested by TTCP partners.

Other Applications Demonstrations

Low Cost Accelerometer Panels: With the concurrence of the ONR Contract Monitor, MSI, NRL, and NUWC (M. Moffett) undertook the development of velocity sensors for potential use in the CAVES (Conformal Acoustic VElocity Sonar) program. The motivation was to exploit the MSI low cost injection molding technology to manufacture the sensors for this application. Several 100 x 100 x 18 mm (4" x 4" x 0.7") panels, each containing 16 net shape molded PZT accelerometer elements, were produced and delivered to NUWC-USRD for evaluation.

Hydrophone Arrays: The objective of this task was to fabricate two, 40 element hydrophone arrays using 1-3 piezocomposite materials for surface ship mine detection applications. The completed arrays were delivered to the Naval Undersea Warfare Center, Newport for evaluation.

2. Accomplishments Versus Objectives

Fine Scale Piezocomposite Synthesis

The basic MSI injection molding process was adapted successfully and new procedures were developed, where necessary, to facilitate molding of extremely fine 1-3 composite dimensions. The 1-3 tooling approach was shown to be capable of achieving dimensions down to at least 50 μm, and that of the 2-2 tooling down to at least 20 μm. MSI demonstrated for the first time that ultrafine scale 1-3 composites could be net-shape fabricated in reusable tooling.

The ultimate 1-3 piezocomposite dimensions achieved were 50 μm diameter PZT rods at 0.25 PZT volume fraction, compared with a program goal of 25 μm rod diameter. For 2-2 piezocomposites, the ultimate pitch dimensions achieved were 45 μm for 0.5 PZT volume fraction, compared with a program goal of 25 μm for this configuration. As the work progressed, it became increasingly obvious that achieving the ultimate goal dimensions would require major effort and that the primary defense and commercial application requirements were for coarser piezocomposites. Consequently, with Contract Monitor approval the technical emphasis for the latter half of the program was redirected away from ultrafine scale dimensions, and on to demonstrating the performance benefits of the fine scale net-shape piezocomposites in imaging and other applications of greater interest to the Navy.

The 1-3 process was successfully scaled up to 30 mm square pieces for PZT element arrays of 100-150 μm diameter rods at 25% PZT volume fraction. This allowed MSI to perform high frequency testing, as well as make samples available for evaluation by the Navy and the private sector. An additional effort, aimed at developing fabrication technology for 1-3 composites having coarser elements in the 200-600 μm range, was pursued. The impetus for this work was based on feedback from the acoustic imaging systems user community which indicated that transducers having PZT elements in that size range were needed for defense and commercial undersea applications in the frequency range 0.5 to 3 MHz. The results of this work provided the technical basis for refinement and scale-up under a subsequent SBIR program (ONR contract N00014-95-C-0117).

The 2-2 work proceeded according to plan. The smallest pitch dimensions produced were 45 μm, smaller than those commonly achieved by conventional dicing. There appear to be markets for such ultrafine scale 2-2 composite transducers in intravascular and endoscopic ultrasound. Applications include both defense (battlefield medical diagnosis and treatment) and commercial uses, especially where low cost facilitates disposable usage. Large area scale-up and manufacturing was pursued under a separate SBIR funding.

Piezocomposite Evaluation

Under the TTCP portion, MSI supplied custom 1-3 hydrophones for evaluation by NRL-USRD and DRA. Using low cost tooling technology developed under contract number N00014-95-C-0117, MSI was able to fabricate 1-3 composites having PZT elements of diamond and triangular-shaped cross-section. These were evaluated at Strathclyde University to help understand interelement mode suppression. In addition, several new types of double layer 1-3 piezocomposite with thickness mode resonance frequencies under 100 kHz were developed, including some that resonated at frequencies as low as 45 kHz. These results were subsequently applied by T. Howarth of NRL-DC under separate funding to produce stacked 1-3 piezocomposites for Navy transmit applications [3].

A new molding technology was used to produce 40 volume percent PZT preforms for frequency applications in the range 250 kHz to 1 MHz. This composite was incorporated into the curved receive array for underwater mine hunting. Two prototype electronically beam steered arrays were fabricated and delivered to UDI for systems integration and test. The first deliverable array (S/N 002) was tested in the outdoor tank at the Navy Coastal Systems, Panama City, Florida. The second will be evaluated in the next phase of the program.

In collaboration with Tetrad Corporation, a high frequency linear array was constructed and tested using fine-scale injection molded 2-2 composite. Images made using the 2-2

composite array demonstrated the excellent quality that would be expected from an array with 85% fractional bandwidth. No unusual behavior or artifacts were observed.

Other Applications Demonstrations

Several 100 x 100 x 8 mm accelerometer panels with integral low noise pre-amplifiers were produced and tested by NUWC-Newport. The first generation panels showed good acceleration sensitivity when tested in air on a shaker table. However, initial in-water evaluation revealed pressure sensitivity that was attributed to strain transmitted to the PZT elements from the circuit board mounting. This has since been verified under the new Smart Panels program (ONR/DARPA contract N00014-97-C-0236).

Two 40 element hydrophone arrays were fabricated, tested in-house and delivered to NUWC Newport for evaluation in shipboard mine hunting applications.

3. Results

Fine Scale Piezocomposite Synthesis

1-3 Piezocomposites

Molding Process Development:

The injection molding process conditions used for fine scale piezoceramic preform fabrication were similar to those reported elsewhere for fabricating coarse scale 1-3 composites [1]. The same wax-based binder system was used for most of the work, except for a brief study of alternative binders which was conducted to determine whether molded part green strength could be improved via polymer additions to the wax binder system. Since the alternative binders tested did not result in any improvement to the molding process, this activity was discontinued after completing the initial studies.

Extending the coarse 1-3 molding process to form composites having ultrafine 1-3 connectivity required adjustments to the green process steps aimed at improving tool cavity filling and molded part ejection. Changes were needed in the areas of powder processing, molding, and molded part ejection, but not in binder removal and sintering. Since all of these process steps were highly interdependent, adjustments made in one area were usually balanced by changes in subsequent process steps, especially binder removal.

Early molding process modifications centered principally around reducing the melt viscosity of the compounded mix through binder modification and optimization of the PZT powder particle size distribution. Mold filling was facilitated by reducing the melt viscosity through PZT solids reduction and increases to the molding temperature. Unfortunately this led to problems with binder bleeding during tool filling which in turn caused uneven filling and part collapse during binder removal. To avoid binder bleeding, the process conditions were adjusted to increase the PZT-binder mix viscosity. This necessitated changes in molding procedures aimed at accommodating the more viscous mixes. These changes included higher pressures and lower temperatures, requiring modifications to the molding equipment. Two experimental molders were designed to allow increased molding pressure, to improve control over temperature, and make larger area devices up to 30 mm square. Approximately 150 runs were completed in this experimental set-up, leading to a greater understanding of the mechanisms of molding and ejection. Using procedures established in prior work, several sets of 1-3 tool inserts were made to test the new

molding procedures and equipment. 1-3 inserts varied in size from 20 to 40 mm square, with cavities designed to produce green PZT elements ranging in size from 50 to 150 μm. After several experimental iterations of molding temperature, pressure and time, complete tool filling was obtained consistently for all of these configurations. Ejection was then studied as a function of temperature, pressure, binder formulation and binder content.

High quality molded parts were obtained consistently for element sizes over 120 μm, despite the increased tool area. In most cases the parts were removed with all elements intact. (Note that for a 30 mm square tool insert, this amounts to approximately 15,000 elements per part.) Problems of element breakage at the corners of the array were eliminated by applying the ejection pressure more uniformly so that all elements were stressed equally during ejection. Figure 1 shows such an array. The aspect ratio of the PZT rods can be seen clearly in Figure 2, where an area of rods was broken off and the rods lie horizontally. The rods were approximately equal in length, uniformly tapered along the length, with an aspect ratio of about 4-5. For very fine element arrays, 50μm in diameter, the yield of intact elements was low. Fracture usually occurred at the point where the elements contact the PZT baseplate, indicating that this was the region of maximum stress during ejection (the tooling is chamfered in this area to minimize this stress). Occasionally rods fractured across the thinner portion of the diameter around their mid-point. The presence and location of intact PZT rods (Figure 3) indicated the feasibility of ejecting this composite configuration.

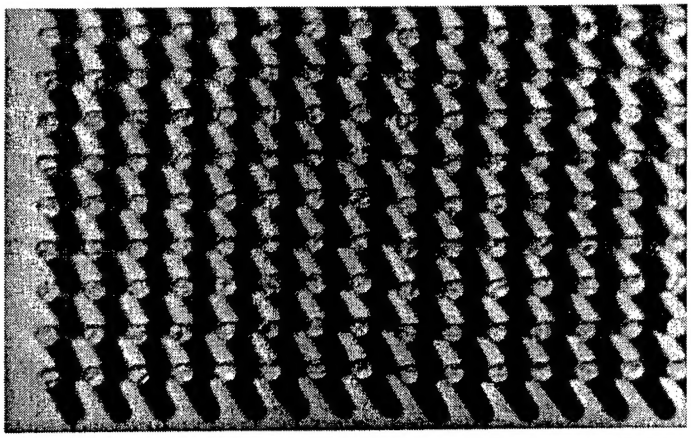

Figure 1. 1-3 composite PZT preform having 120 μm diameter elements.

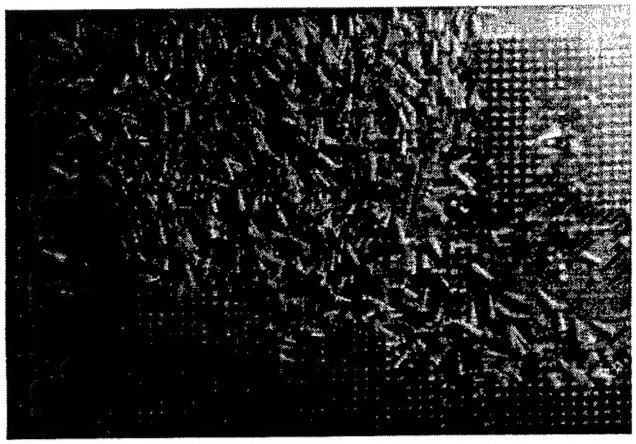

Figure 2. Aspect ratio of PZT rods in a similar composite to Figure 1.

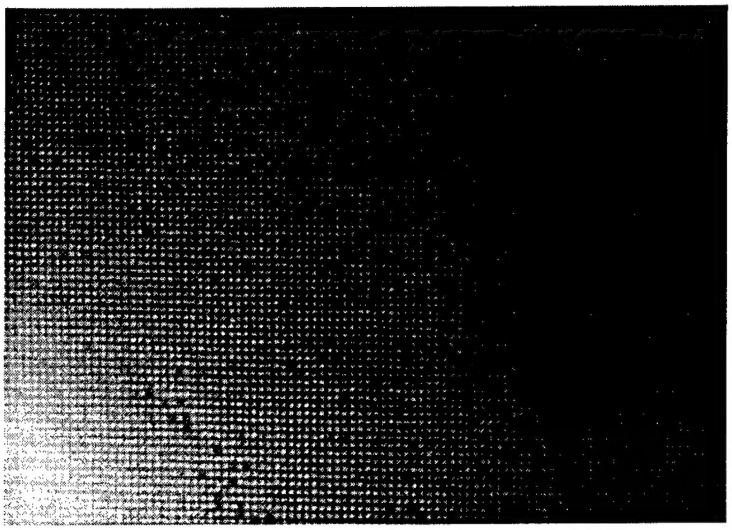

Figure 3. State-of-development 1-3 composite preform, 40 volume % PZT rods, 70 μm diameter.

Other improvements were made to the binder removal procedure. The cross-sections of the in ultrafine scale composite preforms were extremely small, greatly alleviating the problems normally associated with binder removal in injection molded ceramics and allowing much faster burnout cycles. Accordingly, the binder removal mechanism was examined to determine how the various time/temperature stages could be accelerated. A multi-hold cycle involving different heating rates was established, resulting in a decrease in the binder removal time from several days to under 16 hours.

Several challenges with binder removal in high PZT volume fraction composites were solved. Since the elements in these materials were arranged very closely, even small amounts of warpage during binder removal resulted in adjacent elements coming into contact and collapsing. The problem was associated with certain composite features, in particular PZT element aspect ratios in excess of ten, and very fine elements less than 50 μm wide.

Concerns about excessive lead loss during sintering from the high surface area 1-3 preforms proved unfounded, and conventional closed crucible sintering was sufficient to obtain normal PZT-5H ceramic piezoelectric properties in the fine cross-sections.

Tooling Development:

Several iterations of tooling were required before 1-3 preforms could be made reproducibly. These tooling design iterations were conducted on specimens having nominally 150 μm diameter rods. Consequently, devices having these dimensions showed the greatest progress, resulting in the preparation and testing of 1-3 composite specimens which were finished to a high degree of perfection.

The development of tooling to allow intact separation of the green PZT part from the densely packed fine holes in the tool received particular emphasis as part of the process refinement for ultrafine scale 1-3 PZT preforms. In this regard, the degree of taper on the tool cavities proved important in facilitating part ejection. In addition, the tool cavity walls were made as smooth as possible to permit easy sliding of the molded preforms during ejection from the tool. Figure 4 is a scanning electron micrograph of an as-molded PZT

preform having nominally 150 μm rods. As shown by the micrograph, the PZT elements have significant taper and a high aspect ratio. The as-molded rod surface was usually smooth and flaw-free provided the part fully packed out during molding.

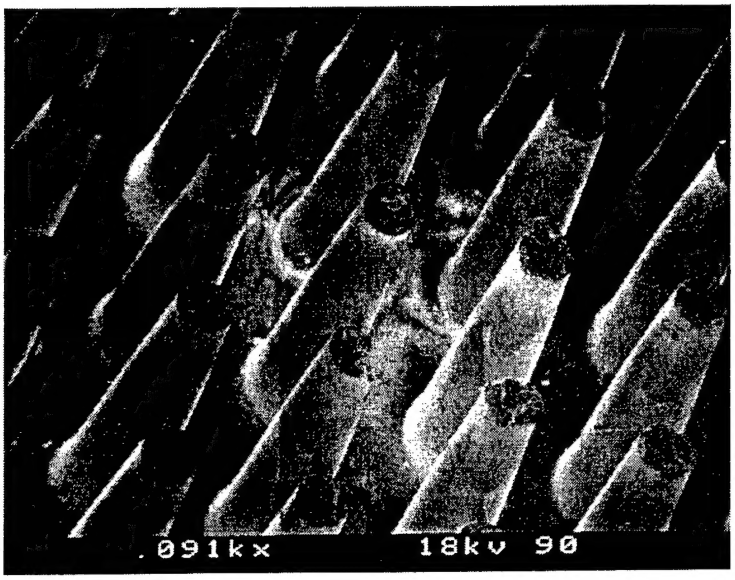

Figure 4. SEM micrograph of as-molded PZT rod array showing the taper and smooth surface finish of green rods.

Establishing process conditions that lead to satisfactory ultrafine scale 1-3 PZT preforms required approximately 200 molding iterations aimed at establishing the trade-offs in temperature, pressure, time, tool geometry and ejection procedure. The major process parameters were sufficiently rugged that procedures for molding 100 to 150 μm PZT rods proved to be highly reproducible. For finer dimensions, the process was verified to be capable of fabricating green PZT rod dimensions down to 50 μm diameter, but with considerably poorer yield and part quality.

Figure 5 shows an early preform in which the outermost PZT rod were severed during ejection, which was believed to be caused by excessive stress on the fibers at the corners of the array as the ejection pressure was applied. The ejection process was refined to enable the complete rod array to be recovered intact. Figure 6 shows a section of an as-molded 1-3 preform having 150 μm diameter rods, approximately 1mm long with a PZT content of 25%. In general, mold filling proved to be very uniform, with each cavity packing out evenly. Figure 7 is a scanning electron micrograph of the surface of a molded rod, indicating the high surface smoothness, which was important for successful part ejection. In Figure 8 the PZT element array was imaged edge-on to illustrate the aspect ratio of these rods, which was approximately 6. Figure 9 shows a general view of a sintered 1-3 array having nominal rod diameter of 120 μm. The as-sintered surface of a PZT rod is shown at higher magnification in Figure 10 where the PZT grain size is seen to fall within the range of 2 to 5 μm, typical for this PZT-5H formulation.

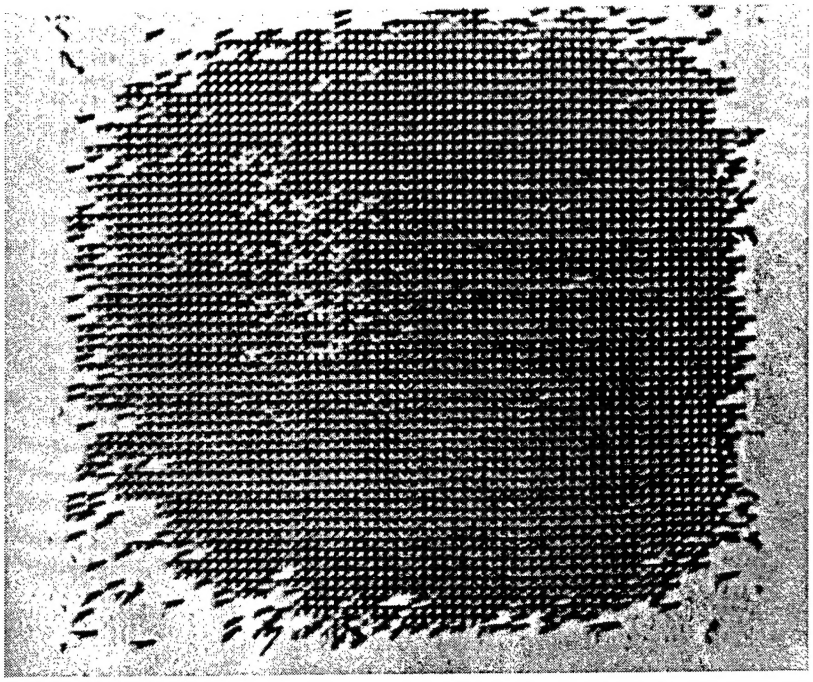

Figure 5. Early as-molded PZT preform having 70 μm diameter rods and 40 volume % PZT. The outermost rods, especially those at the corners, have been severed during ejection from the mold.

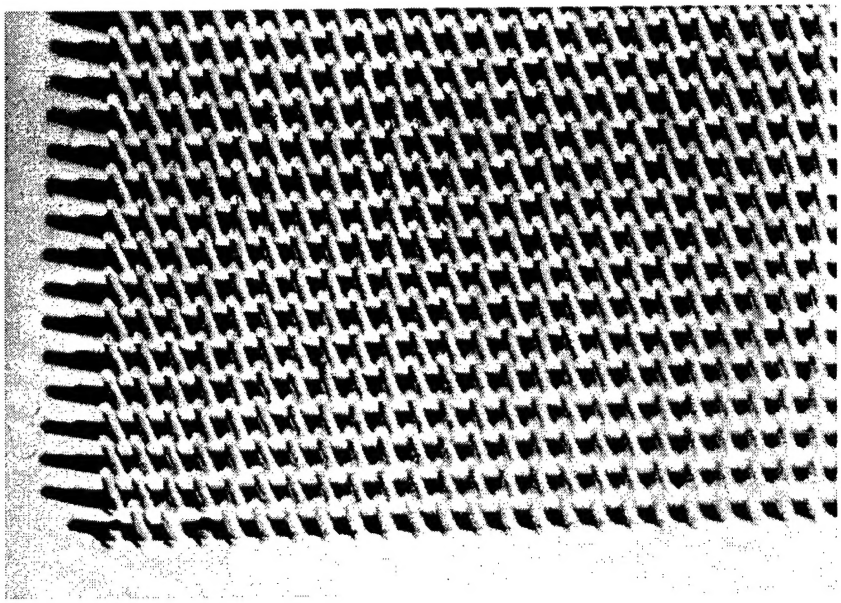

Figure 6. As-molded preform consisting of 150 μm diameter rods, 25 volume % PZT.

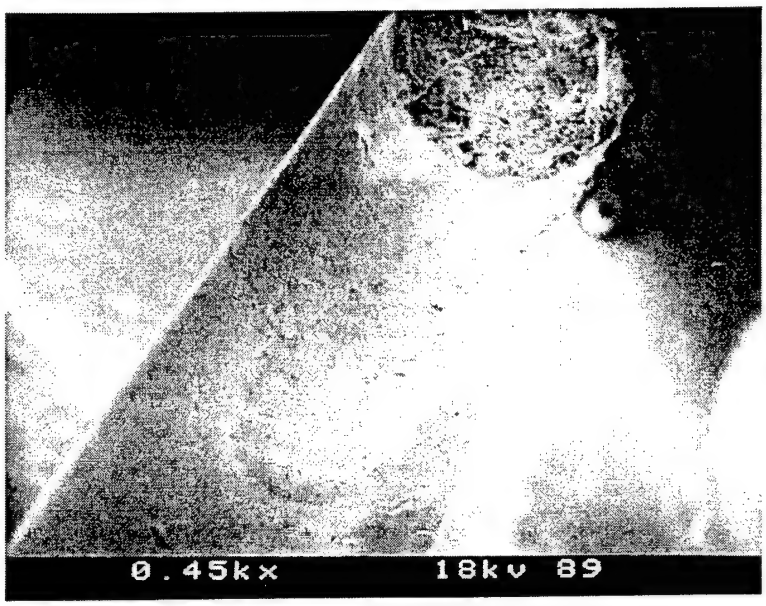

Figure 7. SEM micrograph of 150 μm diameter as-molded PZT rod.

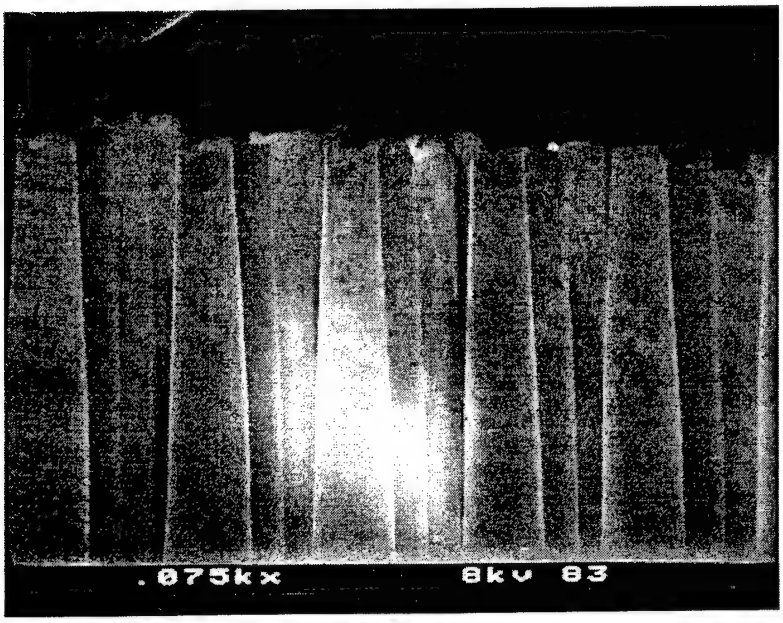

Figure 8. SEM micrograph of green PZT rods, 150 μm diameter, showing the rod aspect ratio (approx. 6).

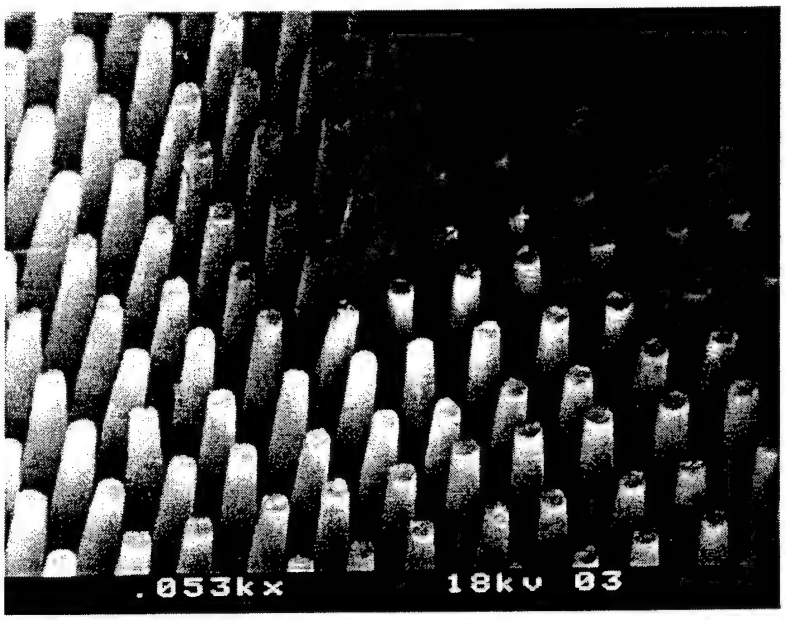

Figure 9. Sintered 1-3 PZT preform having 120 μm diameter rods.

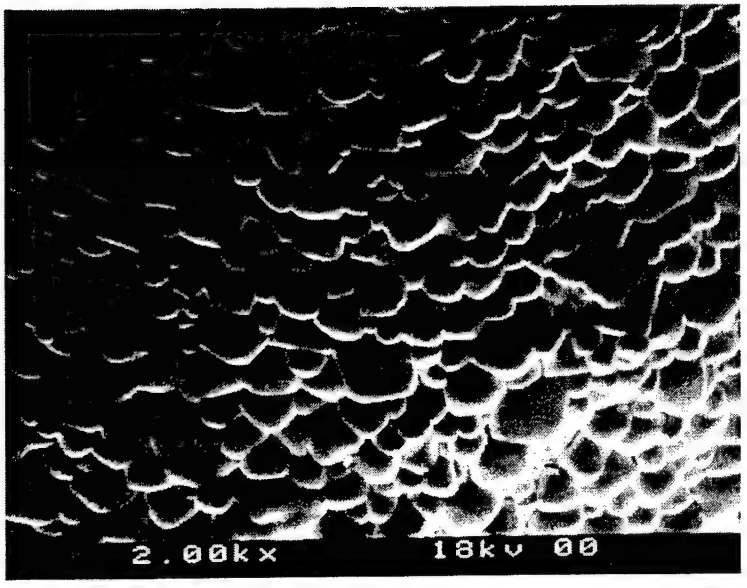

Figure 10. As-sintered surface of PZT rod from Figure 9, showing the PZT grain size.

Figure 11 is an optical photograph of a preform having nominally 70 μm diameter rods and 40% PZT content. After firing (Figure 12) the sintering shrinkage yielded rods that were approximately 40 μm in diameter at the narrow tip and nominally 80 μm diameter at the base. The aspect ratio for these PZT rods ranged from 10 to 12, an extreme level that arose because of the large thickness of the tooling. The effect of this extreme aspect ratio on PZT rod shape is shown on the right in this figure, where one rod has undergone some distortion during ejection from the mold. For production of high quality 1-3 ceramic preforms, a tooling thickness limitation was found corresponding to a rod aspect ratio of approximately 7. Most resonant applications require aspect ratio values of only 3 to 4 to gain the transducer performance benefits of the 1-3 composite configuration. However, in the piezocomposite applications task, it was subsequently found that distortion of the ceramic preform during firing resulted in much of the 1-3 piezocomposite thickness being lost during composite finishing. Therefore, although this aspect ratio would appear to be adequate for most 1-3 piezocomposite applications, higher aspect ratios would benefit the composite finishing operation by allowing for more material to be removed during lapping.

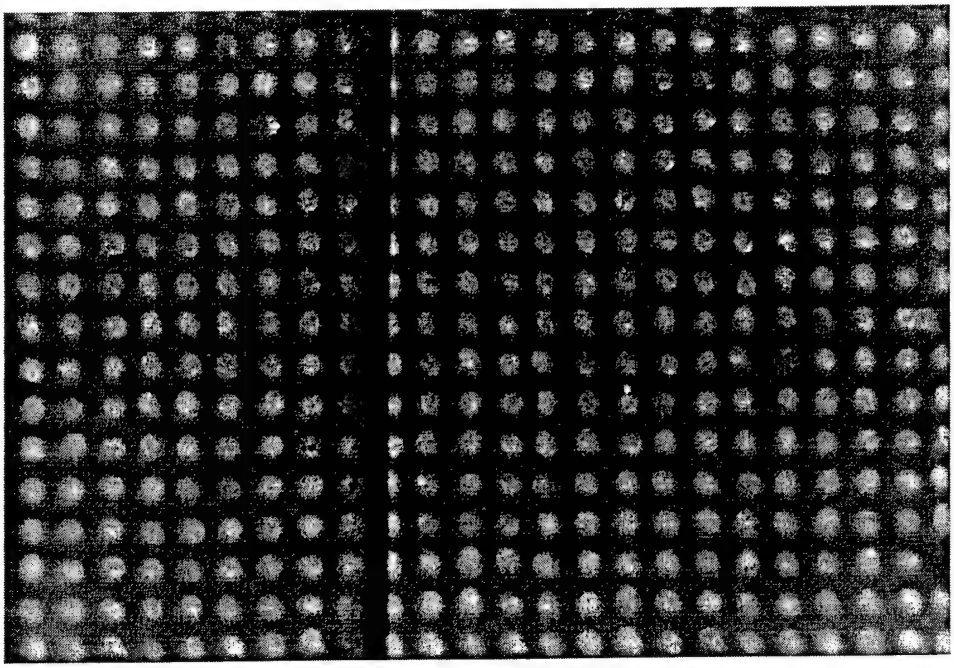

Figure 11. Optical photograph of sintered PZT element array consisting of 70 μm diameter rods at 40 volume % PZT. The human hair in this figure is 60 μm in diameter.

Figure 13 shows the as-sintered PZT surface near the tip of the shortest rod seen in Figure 12. The material was dense and pore-free even though the rod diameter was only 40 μm at this point along its length. Apparently the process was capable of filling very fine dimensions and producing high quality PZT rod arrays of this diameter or less.

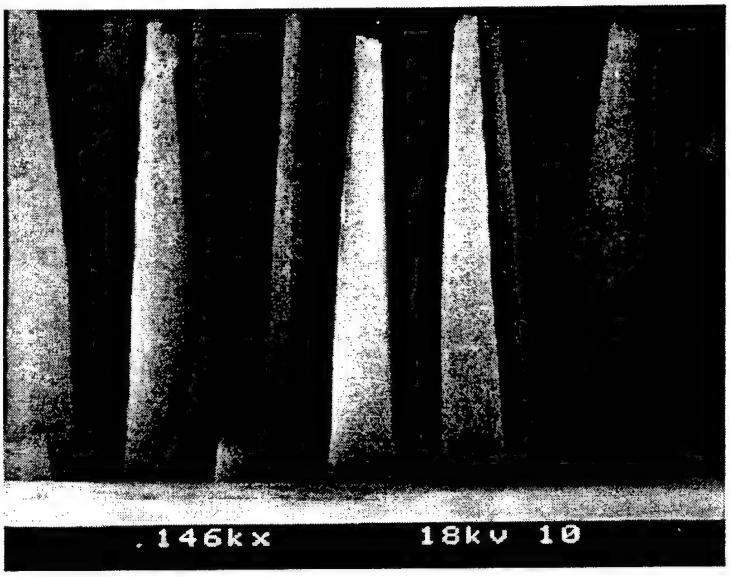

Figure 12. SEM micrograph of sintered PZT rods 70 μm in diameter. The aspect ratio varies between 10 and 12 for these examples.

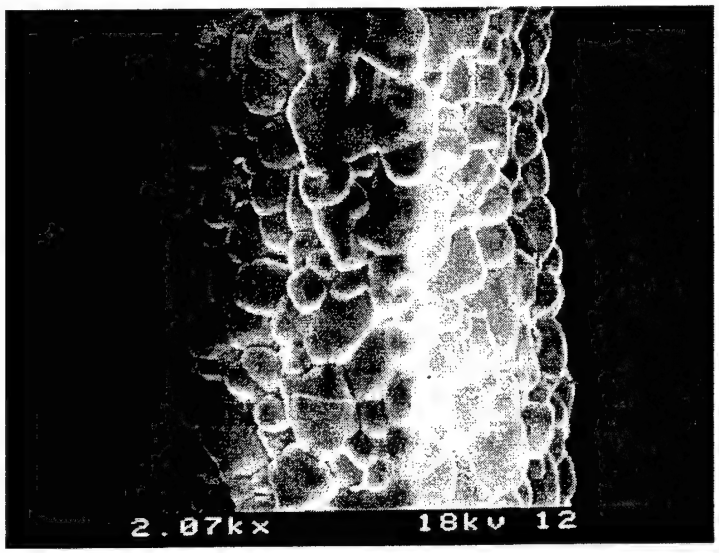

Figure 13. As-sintered surface of the upper portion of a rod from Figure 12. The rod diameter is approximately 40 μm.

Figure 14 is an optical micrograph of a sintered preform that was encapsulated in epoxy resin and sectioned to remove the PZT base and expose the PZT rod ends. Grinding the 1-3 composites without damaging the rods proved straightforward. The efficiency of poling was verified by d_{33} measurements and the change in dielectric constant.

The thickness mode resonance spectra obtained for two 1-3 specimens having sputtered gold electrodes are illustrated in Figures 15 and 16. These resonance curves show considerable distortion, precluding any estimation of the piezoelectric parameters based on these data. For these specimens the thickness was 400 to 450 μm, yielding a PZT rod aspect ratio of approximately 3, sufficient to obtain a clean dilatational thickness mode

resonance. Most probably, the distortion in the resonance curves arose from interelement (lateral) modes occurring near the thickness mode for this specimen thickness, PZT volume fraction and polymer matrix material.

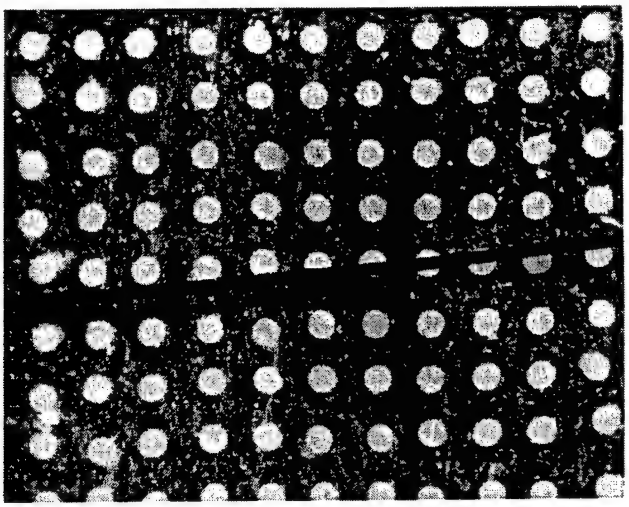

Figure 14. Optical micrograph of finished composite consisting of 120 μm diameter PZT rods in epoxy resin matrix. Reference diameter is 60 μm.

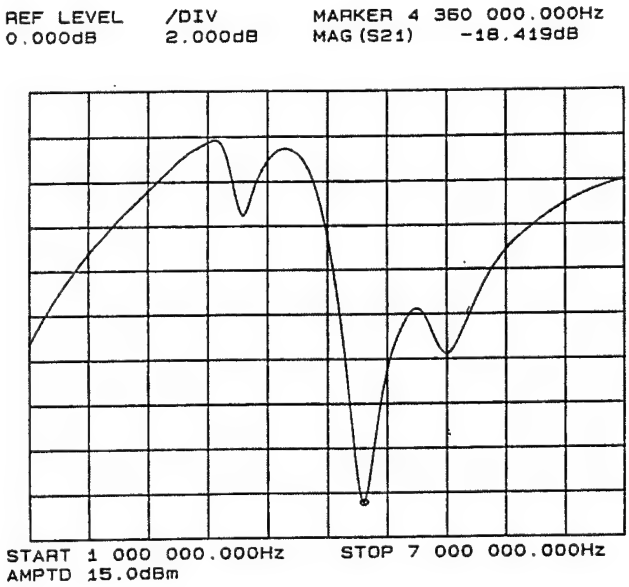

Figure 15. Impedance plot of 1-3 composite shown in Figure 14.

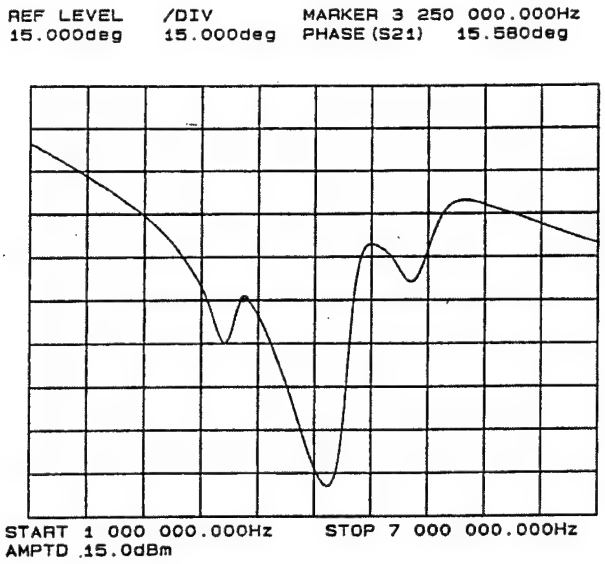

Figure 16. Phase response of sample shown in Figure 14.

Over the course of the program, MSI received numerous requests from both Navy and commercial undersea imaging systems manufacturers for intermediate frequency 1-3 piezocomposites, operating in the 1 to 3 MHz range. As a result of this Navy interest, and after reviewing program priorities with the ONR Contract Monitor, MSI redirected its 1-3 composites effort onto materials having PZT element dimensions in the 200 to 600μm range, rather than pursuing the earlier objective of achieving under 25 μm element dimensions. The new configurations also facilitated 1-3 composite fabrication for the TTCP portion of this program where the requirement was for composites operating in the frequency range 0.25 to 1 MHz.

Several new tool fabrication options were pursued under this program for making intermediate frequency 1-3 transducers, aimed at both reducing tool cost and at achieving appropriate composite dimensions. These 1-3 composite dimensions lay in a difficult process regime, not readily achieved by MSI's standard injection molding tooling approaches. As part of the tooling development activity, the tool application emphasis was focused on improving the tool surface quality to facilitate molded part ejection, while utilizing low cost, readily machined insert materials for tool fabrication. MSI continued these activities under a Phase II SBIR program aimed specifically at developing low cost tooling (ONR contract number N00014-95-C-0117). The materials required for fabricating the TTCP arrays were produced under this program using technologies developed under the related SBIR program.

2-2 Composites:

In the 2-2 composites area, MSI's research emphasis was driven by the need for high frequency 2-2 composites for intravascular and endoscopic imaging applications for both defense and commercial applications. These composites require ultrafine scale PZT element dimensions, i.e. pitches in the order of 35 to 100μm.

Technical efforts aimed at extending the forming process to finer dimensions were particularly successful for 2-2 composites, and PZT element widths below 25 μm were achieved. Using the 1-3 molding equipment and 2-2 tooling, MSI achieved pitch

dimensions as low as 45 μm in 2-2 composites, lower than those commonly achieved reported by dicing. Figure 17 shows a sample of a 50 volume % PZT preform manufactured by injection molding. The PZT features were approximately 22 μm wide, and the individual PZT grains can be clearly seen in this SEM photograph. Several molding vestiges were evident on the as-fired surface, including traces of flash at the upper edges of the PZT strips where the tool inserts contact. There was no evidence that molding or sintering represent barriers to finer dimensions; rather, these are currently limited only by the binder removal process and the availability of suitable tooling. Pitches as low as 20 μm appear feasible, but require fresh tool insert fabrication approaches.

Larger pitches were readily fabricated using this technique (see Figures 18 and 19). The technical approaches identified for 2-2 piezocomposite fabrication under this program were scaled up to large area arrays under the related Phase II SBIR program.

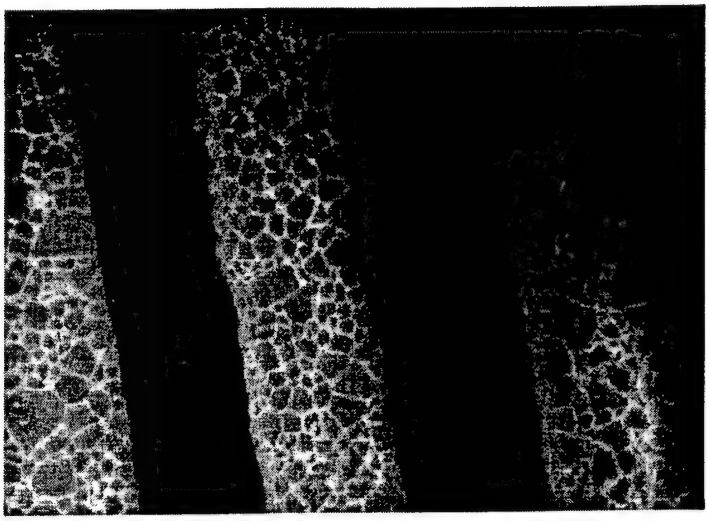

Figure 17. Scanning electron micrograph of as-sintered 2-2 composite preform having 45 μm pitch at 50 volume % PZT content.

Piezocomposite Evaluation

Composite Fabrication and Characterization:

Control of interelement (lateral) spurious resonant modes is critical in both 2-2 and 1-3 piezocomposites. The problem arises when the PZT element dimensions and spacing are such that the thickness fundamental mode frequency coincides with the first and second lateral mode frequencies, which are determined by the polymer matrix properties and the nearest and next-nearest neighbor interelement spacing. The resonance spectrum then becomes a complex mixture of interfering modes in which the advantages of the piezocomposite, viz: high coupling coefficient and low acoustic impedance, are significantly impaired.

Impedance/frequency characterization was utilized to better understand the process and dimensional factors that influence lateral mode generation in MSI composites. The injection molding process has greater flexibility for adjusting these parameters than alternative composite fabrication processes, such as dicing, and was explored in detail with the objective of better control of lateral modes. Several methods for lateral mode suppression

were identified and explored, including modifying the polymer matrix, interelement spacing, element shape, and element dimensions.

To prepare the composite samples for testing, several techniques were developed for incorporating viscous polymer matrix materials into the fine scale sintered PZT preforms. For this purpose, MSI chose polyurethanes, leveraging off experience gained in former Navy contracts to apply this versatile family of materials to resonant composite transducers. These polymers added a new dimension to both undersea imaging and medical ultrasound transducer technology, which then were mainly used only epoxy resins for the composite matrix.

Polyurethanes offered a wide range of stiffnesses, ranging from elastomeric to Shore D-85 hardness, for exploring and controlling interelement modes. They tended to be viscous and cure rapidly, therefore the early technical efforts focused on developing methods for fully infiltrating the materials into the finest 2-2 groove dimensions. Lapping was attempted by outside vendors, but MSI eventually brought this and the electroding process in-house. In spite of the use of gentle lapping procedures, after removing the baseplates on 2-2 samples the lapped devices consistently delaminated at the ceramic/polymer interface. This was resolved by modifying the ceramic surface to improve adhesion, resulting in complete elimination of the delamination problem. Both 1-3 and 2-2 composites became fully lappable with practice, and chrome/gold electrodes were applied with excellent adhesion. Samples for impedance/frequency characterization were prepared in this form.

Lateral Mode Suppression:

Several options exist for controlling spurious modes in piezocomposites. These include:

1. Arranging the PZT elements close together so that the interelement mode frequencies are sufficiently far above the thickness mode to prevent interference. This is the conventional method for interelement mode control used in medical ultrasound and undersea imaging. These composites usually require either high PZT volume fraction and therefore high acoustic impedance, or extremely fine element dimensions that are difficult to fabricate.

2. Arranging the PZT elements to introduce interelement spacing variance. This prevents constructive interference from occurring within the composite at the problem frequencies.

3. Varying the element shape to avoid adjacent facets which may promote cross-coupling between elements.

4. Adjusting the polymer stiffness to reduce cross-coupling between elements. This is effective in suppressing interelement modes, but also adversely affects the thickness mode response by allowing the elements to move independently of the matrix.

5. Modifying the matrix to suppress cross-coupling, while maintaining the surface response uniformity, e.g. by incorporating additives into the polymer matrix phase.

The injection molding process facilitates these options by allowing variations in PZT element geometry and layout. Consequently, MSI explored all of the above approaches under the TTCP portion of this program.

Using modified tooling, MSI succeeded in achieving very high PZT volume fraction in both 1-3 and 2-2 composites (Figure 18). In many cases this exceeded 80 volume percent.

Some versatility in the PZT element shape was also demonstrated (Figure 19). The process offered considerable potential for producing 1-3 and 2-2 piezocomposites in which lateral modes were suppressed. These materials were not fabricated into composites for evaluation of their electromechanical properties because they tended to be too shallow to fill and lap.

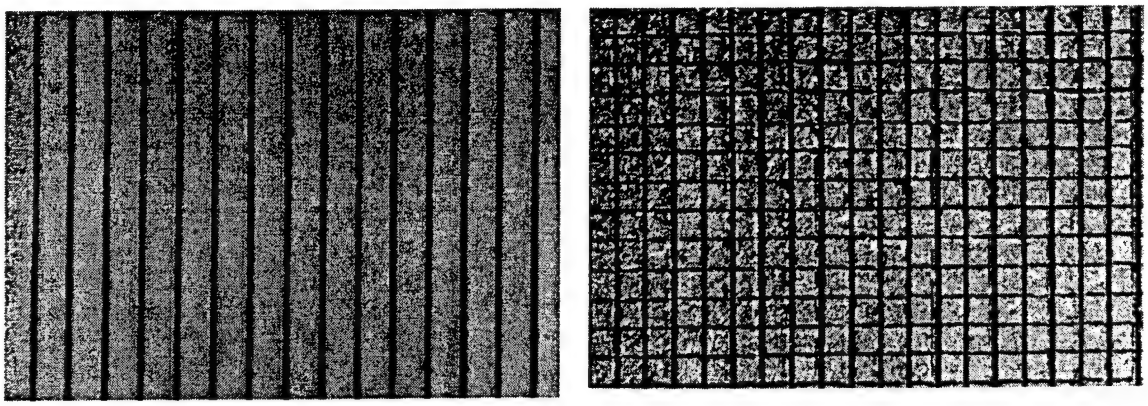

Figure 18. High volume fraction sintered 2-2 and 1-3 piezocomposite PZT preforms (pitch ~150μm).

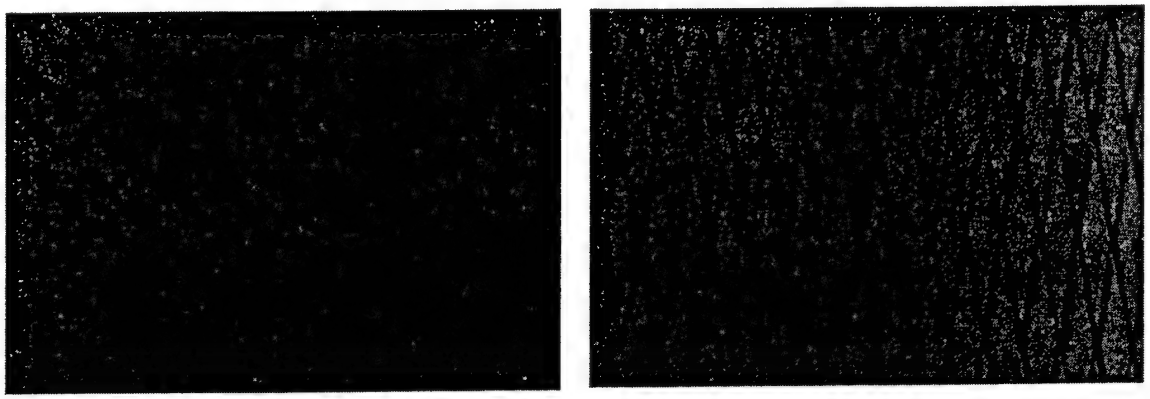

Figure 19. High PZT volume fraction 1-3 composites showing shape versatility of the injection molding process.

Using conventional injection molding tooling, MSI pursued lower PZT volume fraction 1-3 composites (~25 volume % PZT), having various element shapes. For this composite configuration, interelement modes became problematical when the PZT rod aspect ratio was between 2 and 3 for any reasonably stiff polymer matrix. This configuration was, therefore, an excellent choice for examining lateral mode effects, and was adopted as a normalizing standard throughout the work. Figure 20 shows this effect for a 0.5 mm rod array fabricated under related contract number N00014-94-C-0019. Figure 21 shows the nearly ideal thickness mode resonance obtained for the SonoPanel™ configuration developed under contract N00014-92-C-0010. In that case, the PZT volume fraction was 0.3 and the rod dimensions were 1.1 mm diameter by 6.3 mm long (aspect ratio: ~5). The normal soft hydrophone polymer matrix and cover plateswere replaced with a hard (Shore D-80) matrix designed to facilitate uniform resonant response without mass loading. Lateral modes occurred around 500 kHz, well clear of the thickness dilatational mode. The composite configuration in Figure 22 was the same as in Figure 21 except that the material

was thinned to increase the thickness resonance frequency to 1100 kHz, resulting in rods of aspect ratio 1.5. Figure 23 shows the effect of a medium hardness matrix (Shore D-70) in controlling lateral modes. In Figure 23 the composite element dimensions were the same as those in Figure 21, but the spurious resonances were absent. Although this material would not be expected to respond as uniformly as a harder matrix composite, lateral mode responses were minimized, showing the importance of polymer matrix properties on interelement mode generation.

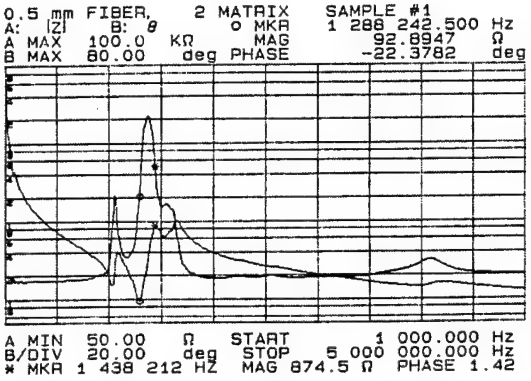

Figure 20. Impedance/frequency characteristics of 0.5 mm diameter rod array, hard polyurethane matrix, 0.25 PZT volume fraction, PZT rod aspect ratio: 2.5.

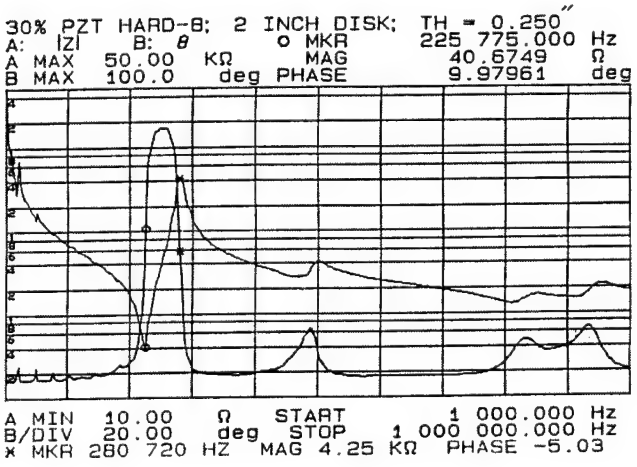

Figure 21. Impedance/frequency characteristics of 1.1 mm diameter rod array, hard polyurethane matrix, 0.30 PZT volume fraction, PZT rod aspect ratio: 5.

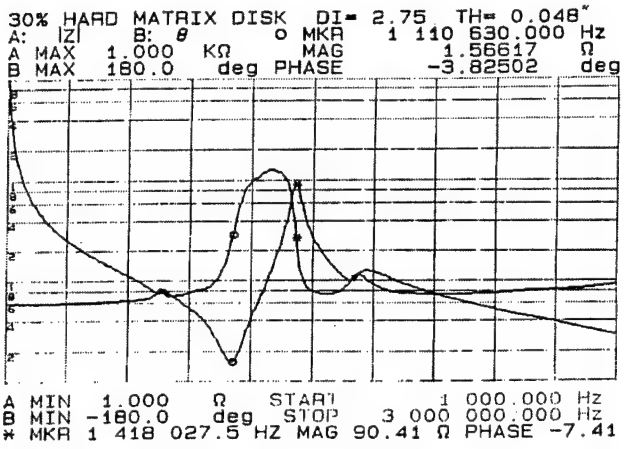

Figure 22. Impedance/frequency characteristics of 1.1 mm diameter rod array, hard polyurethane matrix, 0.30 PZT volume fraction, PZT rod aspect ratio: 1.5.

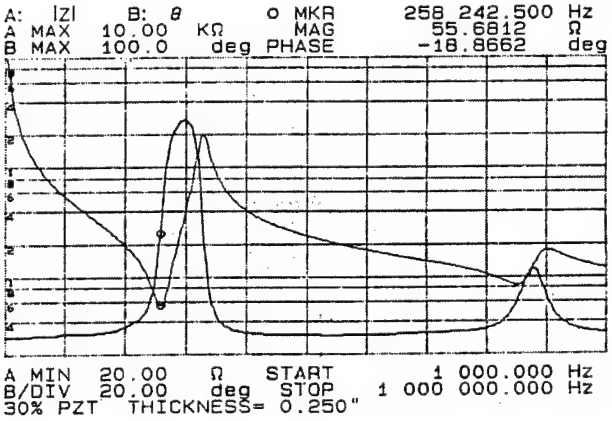

Figure 23. Impedance/frequency characteristics of 1.1 mm diameter rod array, medium-hard polyurethane matrix, 0.30 PZT volume fraction, PZT rod aspect ratio: 5.

Figure 24 shows an alternative design for diamond-shaped PZT elements arranged in a regular array at 25 volume % PZT content. For this configuration there was no overlap of the faces on adjacent elements. However, at higher volume fractions, it can be seen that significant overlap occurs. This composite configuration was built under contract number N00014-94-C-0019 and tested under this program. The as-sintered rod array is shown in Figure 25. The matrix was a hard (Shore D-80) polyurethane which has been shown to clearly support interelement modes in other specimens. Figure 26 shows the impedance/frequency curve for this composite (PZT face dimension: 0.64 mm, aspect ratio: 2.5). There was no evidence for reduced interelement mode resonance in this configuration.

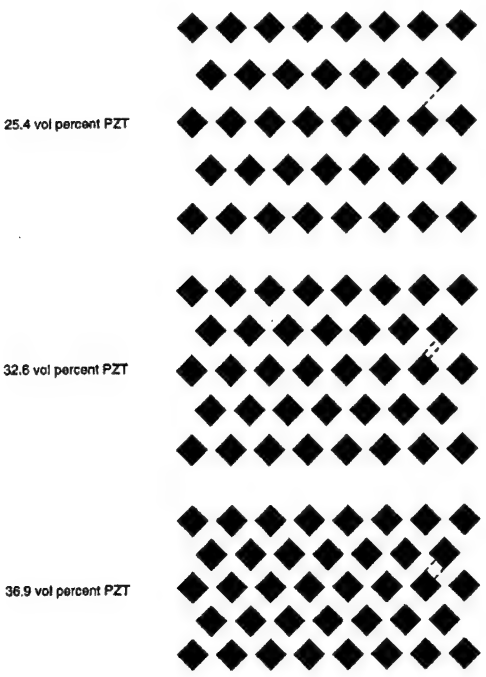

Figure 24. Design for a composite configuration with diamond-shaped elements for exploring interelement mode suppression.

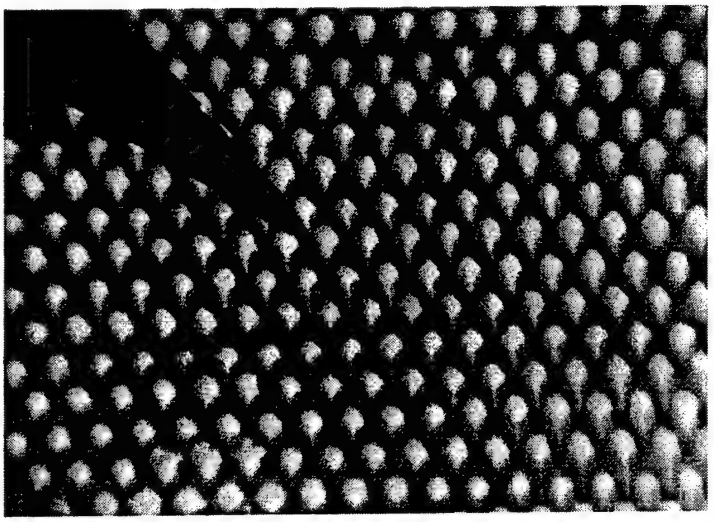

Figure 25. As-sintered PZT preform having diamond-shaped PZT elements.

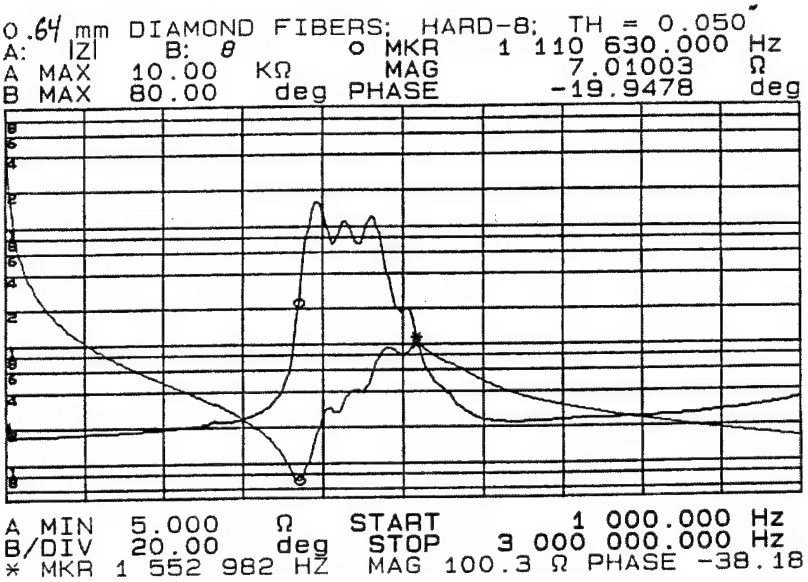

Figure 26. Impedance/frequency characteristics of 0.64 mm square diamond-shaped rod array, hard polyurethane matrix, 0.25 PZT volume fraction, PZT rod aspect ratio: 2.5.

Further work was conducted on triangular-shaped elements designed by Strathclyde University. The Strathclyde design is shown in Figure 27. In earlier work, Strathclyde had observed a significant reduction in interelement mode resonance with this PZT element configuration. However, the Strathclyde composite was assembled by hand-arranging diced triangular elements, resulting in natural variations in the element spacing which could have accounted for the low incidence of interelement mode resonance. In the injection molded version, made under contract number N00014-95-C-0117, the element spacing was more uniform (Figures 28 and 29). Composites were made from the sintered preforms using four different polyurethane matrices: elastomeric, Shore D-80, Shore D-85, and Shore D-80 with polymer microballoons. These were thinned by lapping to 3.25mm (2.5 PZT rod aspect ratio), and tested for interelement modes.

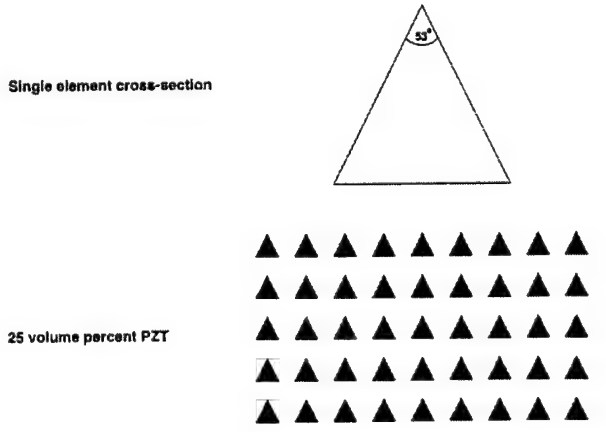

Figure 27. Strathclyde University piezocomposite design using triangular PZT pillars.

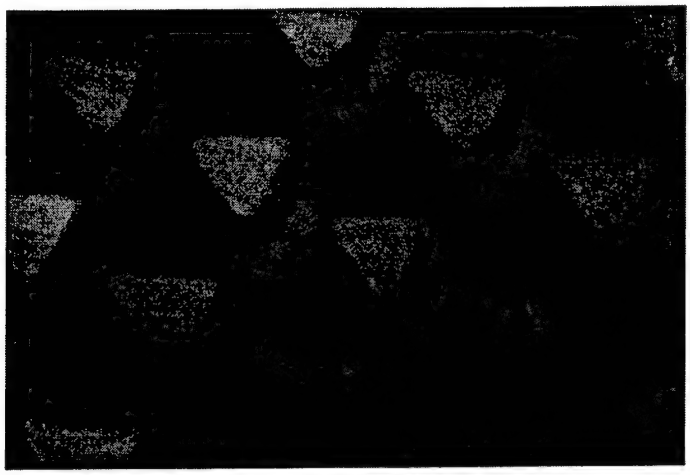

Figure 28. As-sintered array of triangular PZT pillars made under ONR Phase II SBIR Contract Number N00014-95-C-0117.

Figure 29. Triangular PZT pillars in Shore D-80 polyurethane matrix.

Figures 30-33 show the resulting impedance/frequency plots. The elastomeric matrix appeared to have an ideal resonance response because the polymer was so soft that the rods were essentially completely decoupled and resonate independently from each other and the matrix. This material was not functioning as a composite, but rather as an array of discrete piezoelectric ceramic resonators. For the harder matrices, interelement modes were plainly in evidence, even for the matrix containing microballoons. Apparently, for a periodic array of triangular elements, interelement modes were not significantly reduced by the element shape or the presence of uniformly dispersed voids in the matrix.

It appears that the PZT element shape modifications alone did not significantly reduce interelement modes in 1-3 composites. Decreasing the polymer matrix stiffness remains a viable route for lateral mode suppression, but at a penalty in surface response uniformity [4]. An alternative route involves arranging the PZT elements randomly or semi-randomly to control lateral mode generation. The injection molding process is a viable route for the fabrication of such randomized 1-3 arrays. This approach would require further development, but offers considerable potential for suppressing composite lateral modes.

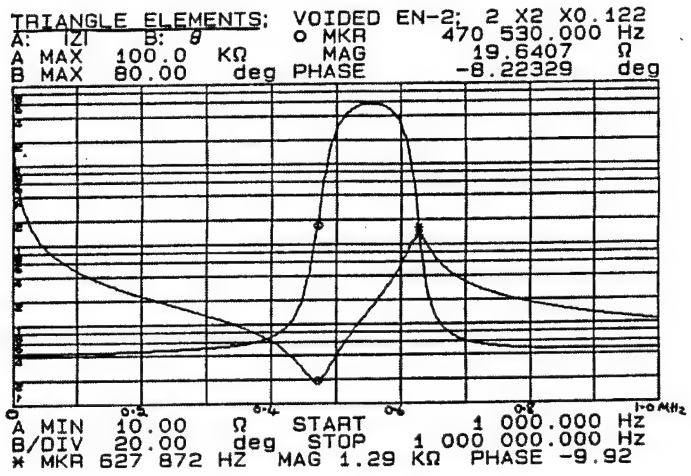

Figure 30. Impedance/frequency characteristics of triangular PZT element array, elastomeric polyurethane matrix.

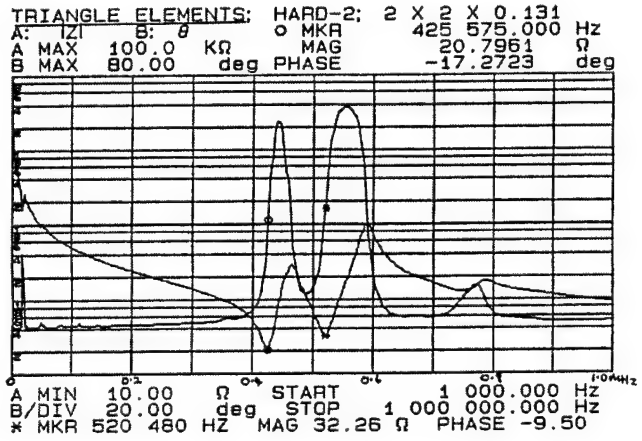

Figure 31. Impedance/frequency characteristics of triangular PZT element array, Shore D-85 polyurethane matrix.

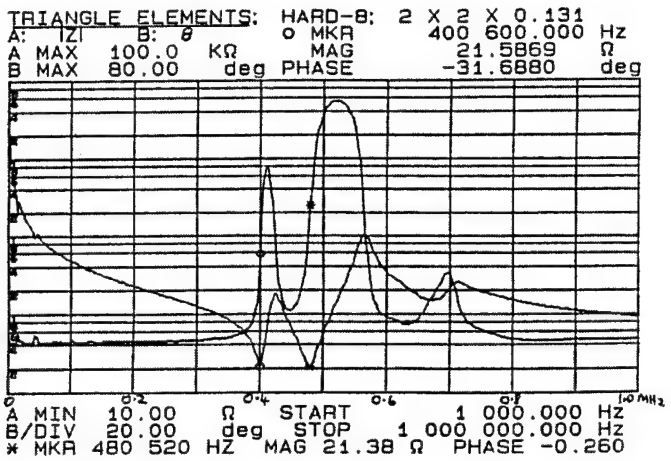

Figure 32. Impedance/frequency characteristics of triangular PZT element array, Shore D-80 solid polyurethane matrix.

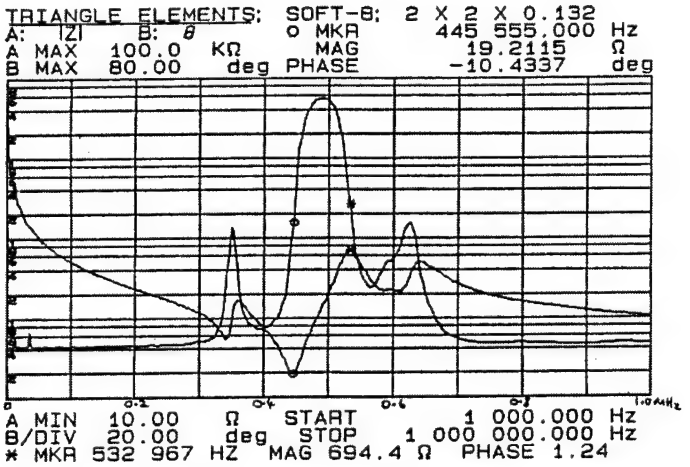

Figure 33. Impedance/frequency characteristics of triangular PZT element array, Shore D-80 polyurethane matrix with voids.

Dice and Fill Array Comparison

Several 45 element injection molded PZT 2-2 preforms having pitch diameters of approximately 150 μm were assembled into composite transducers for evaluation and comparison with conventionally produced arrays. Conventional arrays were diced by Tetrad Corporation from Motorola 3202HD ceramic with similar dimensions to those of the injection molded parts. Several different polymer filler materials were characterized and used to fill the space between the PZT strips. The properties for these materials are given in Table 1.

Table 1. Properties of polymer filler materials used in fabricating the 2-2 arrays.

Material	v_{long} (m/s)	v_{shear} (m/s)	Density (g/cm^3)	Shear Modulus ($x10^{-8}$)	Bulk Modulus ($x10^{-9}$)	Young's Modulus ($x10^{-9}$)	Poisson's Ratio	α_{long} (dB/mm @7.5 MHz)	α_{shear} (dB/mm @2.5 MHz)
MSI Solid 70	2110	728	1.095	5.80	4.101	1.663	0.432	6.6	16.4
MSI Solid 80	2270	966	1.144	10.88	4.472	2.967	0.389	2.1	8.9
MSI Solid 85	2470	1084	1.175	13.81	5.328	3.813	0.381	2.1	11.8
MSI Voided 80	1790	854	0.914	6.67	2.040	1.803	0.353	7.8	9.9
MSI Voided 85	2000	966	0.958	8.94	2.640	2.410	0.348	6.3	11.3
Tetrad Epoxy	2560	1120	1.121	14.06	5.472	3.886	0.382	3.8	6.4
Tetrad Urethane	2425	1050	1.263	13.92	5.571	3.856	0.385	1.35	6.2

Prior to the addition of sputtered gold electrodes, PZT strip, polymer width, and center to center spacing was measured at 12 locations on each device and averaged. Volume fractions were calculated from the measured dimensions. Each composite sample was cut into two rectangular sections; one piece (A) had its longest dimension parallel to the PZT strips with its length >2 times its width, the other (B) had its longest dimension perpendicular to the strips with its length a little longer than its width. The dimensions were chosen so that lowest resonance would not couple to other modes and could be used to measure the sound velocity and coupling to the lateral modes in both dimensions. In each case the smallest lateral dimension was at least 10 times the thickness to prevent interference with the lowest resonant thickness mode.

Capacitance and dissipation were measured at 1 kHz. Resonance measurements were also made using the HP4194A Impedance/Gain Phase Analyzer. Each impedance/phase plot was made over a wide range of frequencies and modes identified. The lowest resonant mode was characterized by the position of the conductance peak (f_r) and the resistance peak (f_a). Coupling constant and lateral velocity (assuming half wave resonance) were calculated using IEEE standards [5]. Similar measurements were made for the thickness mode resonance and the coupling calculated. At the thickness mode resonance, the minimum impedance was recorded for calculating Q_m [6] and the Stopband Edge Resonance (SBER) frequencies were measured at the phase peak as an approximate indicator of their resonance frequency.

Figures 34 and 35 are impedance plots of injection molded and diced-and-filled composites. The two plots were nearly identical. Both composites were made by filling with the same solid 80 polymer and were cut to the B dimensions. In each case the lowest resonance mode (at approximately 130 kHz) was the lateral mode of the largest dimension. Above that, at ~400 kHz, the other lateral mode couples with the third harmonic of the lower resonance. The overtones of these lateral modes died out quickly, so that the thickness mode fundamental was clearly visible between 6 and 8 MHz. Above the thickness mode resonance, SBERs were visible. The highest resonance seen at ~25 MHz was the third harmonic of the thickness mode.

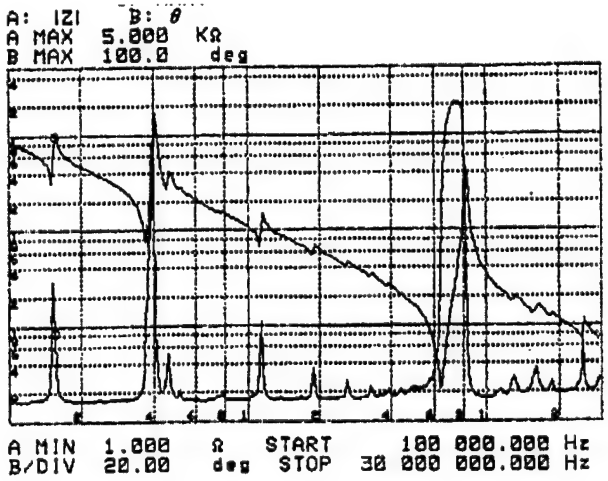

Figure 34. Impedance plot of a 2-2 injection molded composite.

Close examination of the impedance plots showed that the lateral modes in the directions perpendicular and parallel to the PZT strips were nearly identical for the injection molded and the diced samples. As expected, the coupling in the direction of the strips was substantially larger than in the perpendicular direction. Figures 36 and 37 are impedance plots of the thickness modes for an injected molded composite and a diced sample cut in the B dimensions. The slight rounding of the phase plot on the resonance (left) side was due to the thin electrodes used for characterization. Several samples were coated with additional electroplated electrodes, but the coupling constant values measured before and after coating were unchanged.

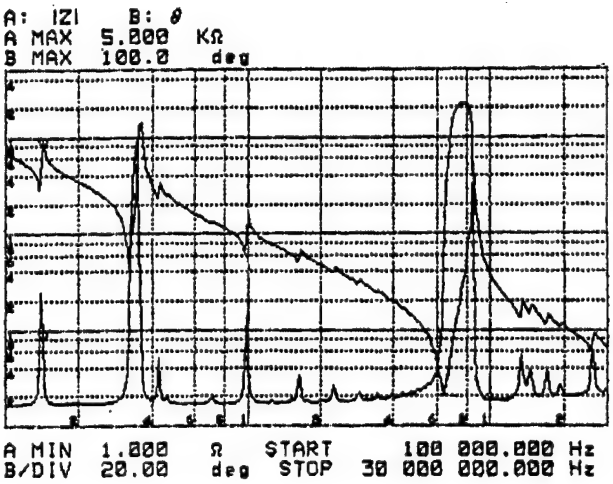

Figure 35. Impedance plot of a diced-and-filled 2-2 composite.

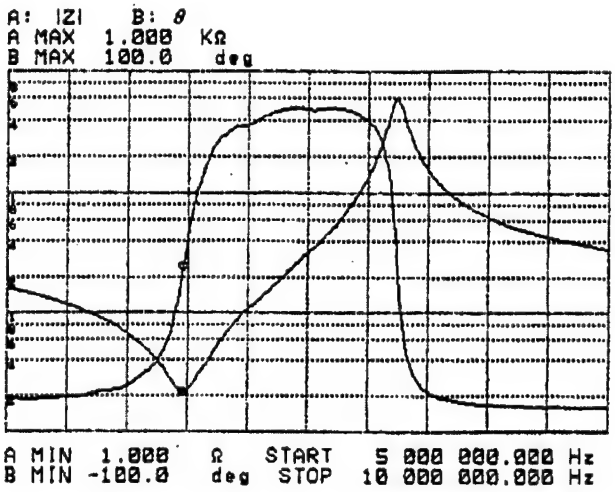

Figure 36. Impedance plot of the thickness mode resonance for an injection molded composite.

Two major SBERs corresponding to the two major SBERs expected in 2-2 composites were seen in the impedance plots (Figures 34 and 35). The lower SBER is associated with a lateral longitudinal resonance of the ceramic strip and the upper one was associated with the lateral shear resonance of the ceramic [7]. The predicted lateral resonance for sample #1 was 12.2 MHz and the predicted shear resonance was at 16.3 MHz which are nearly identical to the measured values. The resonances in the diced samples, while less strongly coupled, appeared to be more distinct.

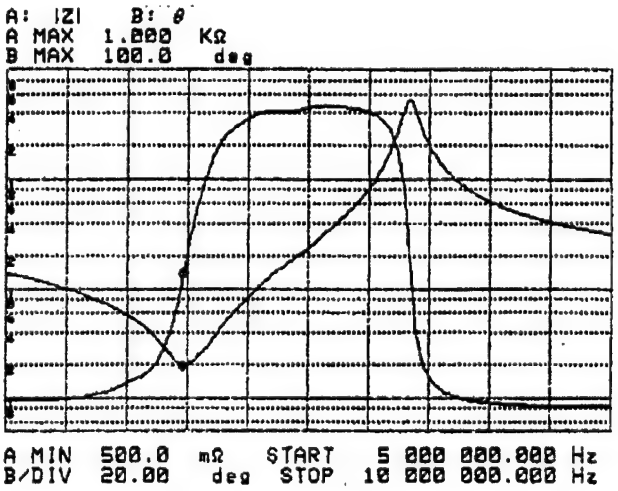

Figure 37. Impedance plot of the thickness mode resonance for a diced-and-filled composite.

Table 2 is a summary of the data for all samples measured. The coupling constant, k_t, and velocity in the z dimension (v_Z) were calculated only for the 3202HD ceramic and solid 80 polymer, but the other fillers and ceramic were similar enough that these values could applied to those cases as well. The predicted k_t ranged from 0.686 at 73% volume fraction to 0.671 for 83% volume fraction. The v_Z ranged from 3.989 mm/μs at 73% volume fraction to 4.062 mm/μs at 83%.

The injection molded composites performed very well when compared to the dice and fill samples. The best samples were within 2% of the predicted k_t. In general, the injected molded samples had slightly lower k_{31} values and less distinct SBERs which are advantageous features for thickness mode transducers.

Table 2. Summary of measured properties of injection molded (mold) and dice-and-fill (diced) transducers.

Sample	Fab.	Filler	vol %	K	ρ (g/cc)	k_t	v_z (mm/μs)	Qm	k_{31}	v_x (mm/μs)	k_{32}	v_y (mm/μs)
1	mold	80	82.9	2384	6.463	0.66	4.063	18.2	0.351	2.98	0.208	1.716
2	diced	ureth	72.8	2343	6.031	0.66	4.246	14.4	0.386	2.86	0.194	1.703
3	mold	80	80.7	2439	6.355	0.66	4.024	18.6	0.33	2.93	0.238	1.671
4	diced	epox	74.8	2520	6.067	0.65	4.047	5.5	0.299	2.85	0.202	1.682

128 Element Array Fabrication and Test:

The objective for building the 128 element array was to compare the processability and image quality of an injection molded composite array with a dice and fill array. Unfortunately the injection molded composite chosen for array fabrication did not match any dice and fill arrays being fabricated by Tetrad. A head to head comparison was therefore not possible. Tetrad selected a 3.0 MHz linear sequenced array that it was building for another customer as the test vehicle for this composite. The nominal specifications for the array are given in Table 3.

Table 3. Array specifications.

Property	Value
Nominal Center Frequency:	3.0 MHz
Number of Elements:	128
Pitch:	0.35 mm
Elevation Width:	18 mm
Geometric Focal Depth:	90 mm

The injection molded composite material had a nominal polymer width of 75 μm and a nominal ceramic width of 125 μm. Using the criterion that the polymer width should be smaller than 0.25 of a polymer shear wavelength, it was determined that the operating frequency should be less than 3.2 MHz.

The array was designed for steering at the edges to produce a trapazoidal image. Tetrad's imaging system is not capable of this mode. This made the total array length somewhat shorter than normal for a 3.0 MHz array yielding an image that was long and narrow. The small pitch (which was still large enough to require subdicing) also yields aspect ratios that are less than ideal for 3.0 MHz. Because of these considerations, Tetrad decided to use the same array geometry but to push the frequency as high as reasonably possible. The higher frequency is more appropriate for an unsteered array of this length and the use of thinner composite improves the aspect ratio.

The initial composite received from MSI was a 1" x 2.25" x 0.015" sample filled with MSI EM/R20 filler. This sample was electroded and cut to array dimensions by Tetrad. Upon careful inspection, a crack was discovered in the composite extending between the

ceramic and polymer for some distance and then across the polymer. This made it unusable for an array.

Subsequently, MSI provide Tetrad with an unfilled 2-2 composite preform. Tetrad filled the composite using the material that had been developed for dice-and-fill composites, ground the sample to thickness, applied a chrome/copper electrode and cut it to size. The properties of the filler are given in Table 4 and the physical dimensions of the composite in Table 5.

Table 4. Properties of the Tetrad filler material.

Property	Value
Longitudinal Velocity	3.02 mm/μs
Longitudinal Attenuation	1.0 dB/mm @ 6.5 MHz
Shear Velocity	1.54 mm/μs
Shear Attenuation	3.7 dB/mm
Density	1.161 g/cc

Table 5. Measured dimensions of the array composite.

Parameter	Value
Mean polymer width	89 μm (0.0035")
Mean ceramic width	133 μm (0.0052")
Mean center-to-center spacing	222 μm (0.0087")
Ceramic volume fraction	60%

The higher shear velocity of the Tetrad polymer allowed the composite to be pressed to a design frequency of 4.4 MHz. Based on Tetrad design criteria the composite was ground to a thickness of 0.345 mm and cut to the final dimensions of the array. The composite was sputtered with a thin layer of chrome (exact thickness was not known) and vapor-coated with a thin layer of copper (thickness also not known). The copper thickness was increased to approximately 1.3 μm by electroplating. The wrap around ground was isolated by cutting just through the electrode with a dicing saw. The composite was poled in air using an E field of approximately 7600 V/cm.

The properties of the composite were measured using an HP 4194 Network Analyzer and are shown in Table 6.

Table 6. Properties of the composite.

Property	Value
K_t	0.611
Q_m	16.3
Relative free dielectric constant	2351
Stiffened velocity (m/sec)	4056
Density (kg/m^3)	4940
Acoustic Impedance (MRayls)	20
Lowest Stop Band Edge Resonance Frequency (MHz)	8.0

The performance was within the range of dice-and-fill composites which often range in coupling between 0.60 and 0.64.

The basic structure of the array can be seen in Figure 38.

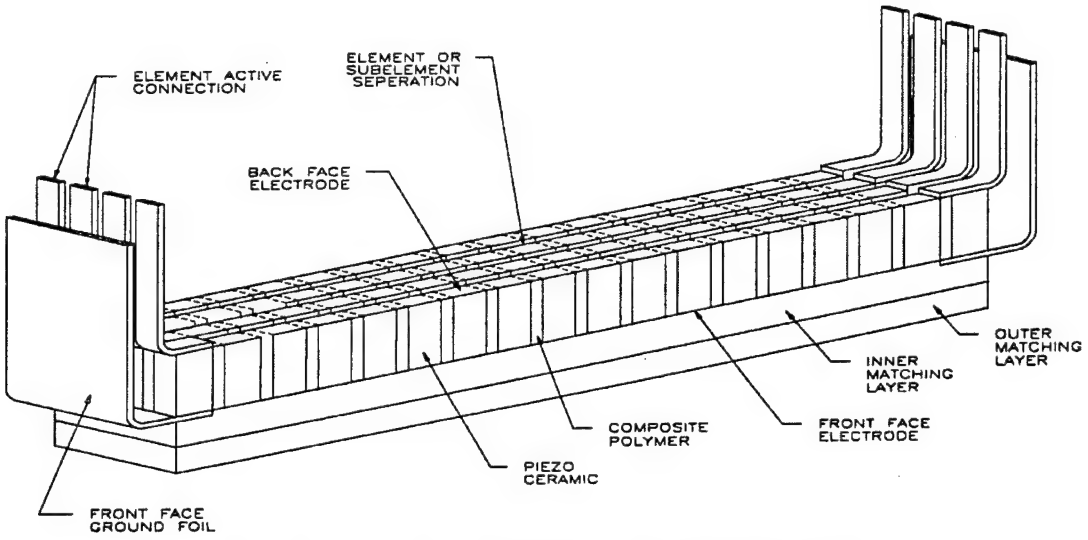

Figure 38. Diagram of an array made using 2-2 composite.

The array was constructed by Tetrad using their standard fabrication techniques. The array dimensions are shown in Table 7.

Table 7. The physical dimensions used in the construction of the array.

Property	Value
Kerf Width (cross dice):	0.0394 mm (1.55 mils)
Crystal Thickness:	0.345 mm (13.6mils)
IML Thickness:	0.142 mm (5.6mils)
OML Thickness:	0.109 mm (4.3mils)
Dicing Depth:	0.569 (22.4 mils)

The composite was electroded with a "wrap-around ground configuration." The ground electrode covered the entire outer face of the composite, connected to electrode material on the long sides, and wrapped to cover a small part of the inner face. An unelectroded section separated the ground from the active part of the electrode that covered most of the inner face. The strips of the 2-2 composite were arranged so that they extend the length of the array. The isolation between hot and ground electrodes was along the strips running the full length of the array on both sides of the composite. (This wrap-around ground is not shown in the figure.)

The outer face of the composite was bonded to the double matching layer system (referred to in the figure as the inner [IML] and outer matching layers [OML]) which was attached to a dicing block. Table 8 lists the properties of the matching layers.

Table 8. Bulk matching layer material properties.

Property	Value
IML Longitudinal Velocity	3.14 mm/μs
IML Longitudinal Attenuation	1.8 dB/mm @ 7.5 MHz
IML Shear Velocity	1.39 mm/μs
IML Shear Attenuation	1.8 dB/mm @ 2.25 MHz
IML Density	2.43 g/cc
IML Acoustic Impedance	7.6 MRayls
OML Longitudinal Velocity	2.4 mm/μs
OML Longitudinal Attenuation	2.6 dB/mm @ 7.5 MHz
OML Shear Velocity	1.05 mm/μs
OML Shear Attenuation	5 dB/mm @ 2.25 MHz
OML Density	1.11 g/cc
OML Acoustic Impedance	2.66 MRayls

The stack of three materials was diced on the dicing saw with the outer composite face on top. The height of the blade was adjusted to leave approximately 27 μm of the outer matching layer undiced. The dicing pitch was exactly one half of the element pitch leaving two layers. (The figure shows dicing through the composite only.) At this point, the composite had small pillars making the structure similar to that of a 1-3 composite.

Flex circuits with metal leads extending past the polyimide were soldered to the inner face of the composite. This was done in such a way that each flex lead tied the two subelements together. All odd numbered elements were connected by a flex circuit on one side of the array and all even numbered elements were connected by a flex circuit attached on the opposite side. A filler material was then placed in the cuts to improve the mechanical stability of the array. The wrap-around grounds, which were separated into pieces by the dicing process were soldered back together using a buss wire.

A premade backing material was bonded to the inner face of the composite in such a way that the solder joints were then embedded and protected. The flex circuits were folded 90 degrees to exit at the back of the array and the ground connection was made to the back of the flex circuits. A silicone lens was cast onto the face of the array and the entire assembly was potted into a plastic housing. A cable with a system connector was attached to the exposed flex circuit leads and the final case was placed over the entire assembly and bonded into place.

The first array completed had 127 working elements with four that were 4 to 10 dB low in amplitude. This is a good result for an initial run with a new material. The performance was very good. A summary is given in Table 9.

Table 9. Array performance.

Property	Value
Mean Center Frequency	4.18 MHz
Mean 6dB Bandwidth	3.32 MHz (79.5%)
Mean -6dB Pulse Length	0.3 μs
Mean -20dB Pulse Length	0.73 μs
Total Variation (excluding problem elements)	3.1 dB
Focal Length (flat Plate)	88 mm

The time waveform and spectrum of a typical element is given in Figure 39.

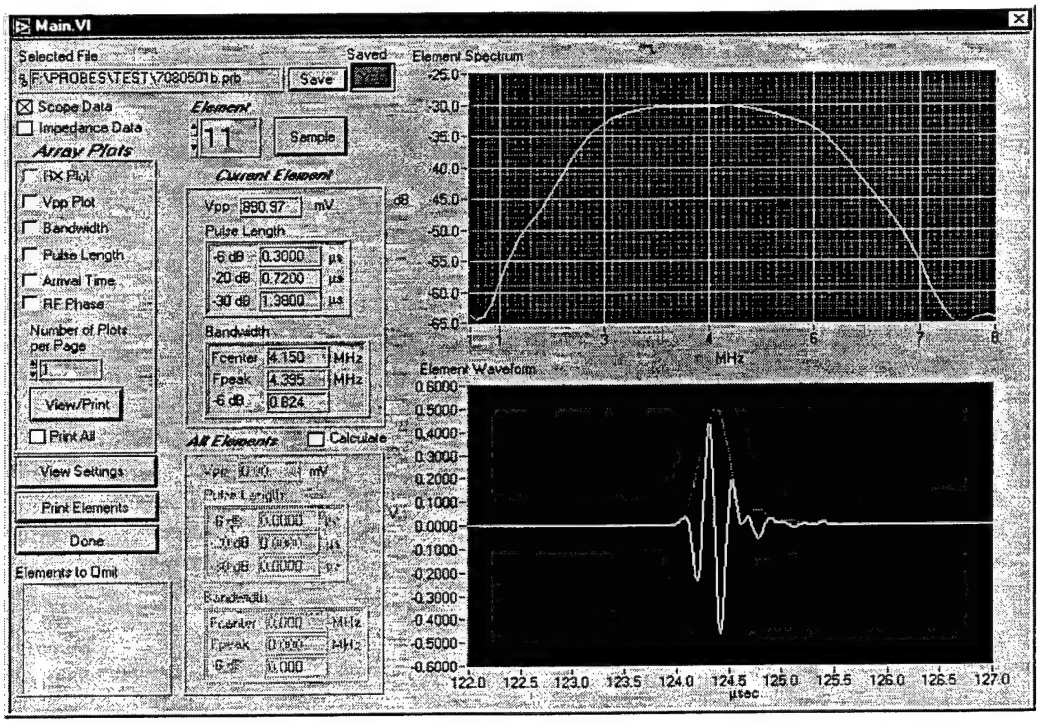

Figure 39. Typical time waveform and spectrum from the composite array.

The relative comparison of the composite array to the ceramic array is shown in Table 10.

Table 10. Comparison of the composite array to the ceramic array.

Parameter	Composite Array	Ceramic Array
Center Frequency	4.18 MHz	3.06 MHz
Fractional Bandwidth	79.5%	67%
-6 dB Relative Pulse Length	1.25 Periods	1.28 Periods
-20 dB Relative Pulse Length	3.1 Periods	2.42 Periods
Sensitivity ref (120 V impulse)	-66.6 dB	-67.7 dB

The composite array was superior to the ceramic array in every parameter except –20 dB Relative Pulse Length. This was probably due to the fact that the matching layers for the composite were not optimized. The sensitivity comparison is slightly misleading. The lower ceramic volume fraction in the composite array would ordinarily lead to higher electrical impedances and an apparent loss of sensitivity. In this case the increase in center frequency compensated this effect so that the electrical impedances were comparable.

The array was integrated into the Tetrad 2200 system and phantom images were made. Typical phantom images are shown below as Figures 40 through 42. The ceramic array did not have a connector that was compatible with the Tetrad 2200 so comparative imaging was not done. Even if it had been done, the difference in center frequency would have made the results difficult to compare. Tetrad's primary imaging engineer however has had many years of comparing images from various arrays and concluded that the image quality produced by the array was excellent. This is consistent with the test results given above.

Figure 40 shows that the probe penetrates to the bottom of the RMI 414B while still achieving good resolution in the near field. Figure 41 demonstrates good axial and lateral resolution throughout the image. Figure 42 shows excellent axial and lateral resolution in the near field.

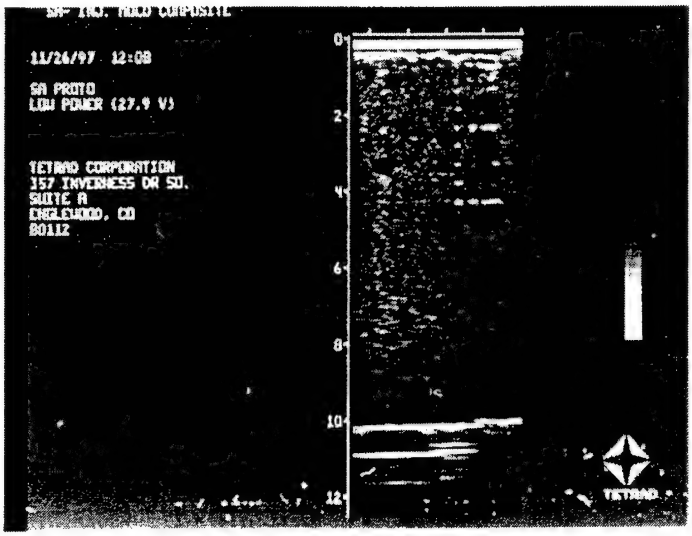

Figure 40. Phantom view showing penetration.

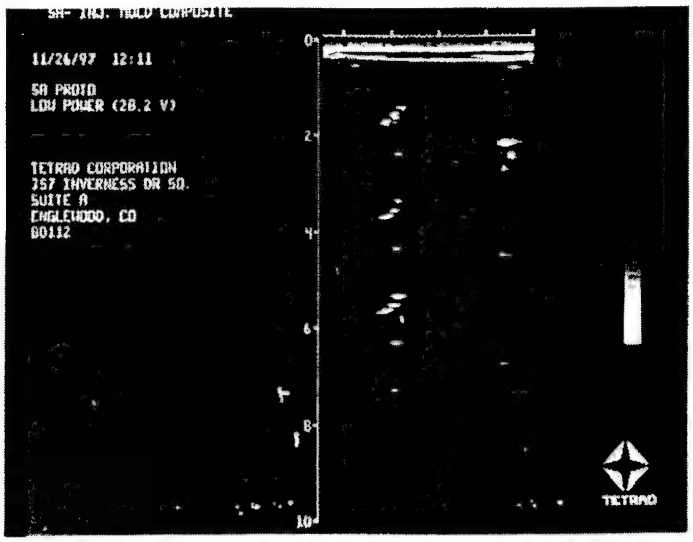

Figure 41. Phantom view showing resolution throughout the image.

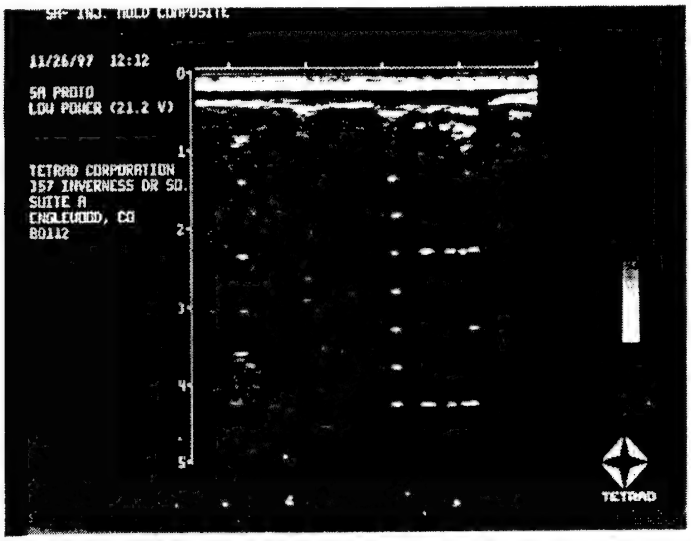

Figure 42. Phantom view showing good near field resolution.

The conclusion of the study was as follows:

1. Injection molded 2-2 composites can be made with performance equivalent to the best dice-and-fill 2-2 composites.
2. Injection molded materials can be easily processed by using the same care and precautions required for handling 2-2 composites.
3. Arrays can be constructed using injection molded 2-2 composites that display exceptional bandwidths (approximately 85%, -6dB round trip) and sensitivity comparable to ceramic arrays if the effects of electrical impedance mismatch are compensated.
4. Images made using the 2-2 composite arrays demonstrate the excellent quality that would be expected from an array with 85% fractional bandwidth. No unusual artifacts were apparent.

TTCP Piezocomposites:

In conjunction with other TTCP groups, MSI participated in three Technical Cooperation Program activities: hydrophones, stacked transducers, and mine-hunting arrays. The TTCP participants were:

- Canada: Royal Military College (RMCC): Piezoelectric measurements.
- UK: Strathclyde University (SU): Piezoelectric composite modeling, design and testing.
  Fugro-UDI (UDI): Undersea array integration and system testing.
  DRA: Hydrophone testing.
- USA: NRL-USRD: Testing, input on US Navy needs.
  Weidlinger Associates (WA): Modelling.
  Ultrex (formerly UltraSound Solutions): Undersea array design.
  Materials Systems Inc. (MSI): Materials design and fabrication.

After several meetings and some revision of the program plan, the collaboration became fully operational in all three technical areas. The plan took into account the differing defense needs of the various countries to the extent possible within the available timeframe and funding constraints.

Hydrophones:

1-3 piezocomposite hydrophones are of considerable interest to the UK Navy for flank arrays, and therefore significant effort was devoted to modelling, fabricating, and testing MSI SonoPanel configurations for this application. In the first six months of effort, MSI supplied two encapsulated 75 mm SonoPanel transducers to DRA. These were RVS tested at low frequency (~50 Hz) and found to have -185 dB re 1V/μPa sensitivity, the same as that measured at 1-100 kHz on 100 and 250mm samples. Since then, two more samples were supplied to DRA for followup testing. These were demonstrated to have flat response within ± 2dB over the frequency range 10Hz to 80kHz.

Strathclyde University performed modelling of the hydrophones as part of their TTCP commitment. MSI supplied data and design parameters to both SU and WA for modelling purposes. The only data that were not available were the mechanical properties of the GRP cover plate materials. To circumvent the problem, MSI made a special 100 mm SonoPanel transducer with aluminum cover plates because it was easily modeled. Results from USRD indicated that this device had interesting resonance behavior and its bandwidth was significantly wider than that of GRP cover-plated devices. The hydrophone data and conclusions were detailed in a separate TTCP report submitted by Strathclyde University to ONR and DRA.

USRD has devoted considerable effort to evaluating the resonance/frequency behavior of encapsulated SonoPanel transducers. A spurious resonance was noted in unencapsulated devices at 100 kHz, lower than the thickness dilatational mode (~220 kHz) for the composite core material. This may have been a mass-loaded thickness mode resonance that corresponded to that of the entire cover-plated stack. Upon encapsulation, the spurious mode resonance frequency dropped to approximately 70 kHz when measured in air. When immersed in water, the 70 kHz mode shifted back to 100 kHz, indicating that the encapsulation material was acoustically-transparent at this frequency, and the

transducer was resonating like an unencapsulated device. USRD and MSI pursued this with WA and SU in an attempt to better characterize the resonance mode and improve RVS and TVR performance uniformity. Details of the characterization work were reported separately by USRD.

In related activity, MSI supplied samples of encapsulated and unencapsulated soft matrix materials to RMCC for acoustic characterization. This proved difficult due to the highly absorbing nature of the EN2 matrix, and characterization of this material was discontinued. However, characterization of harder matrix was performed. To achieve this, MSI built a complete set of 1-3 composite samples having solid Shore D80 matrix in the standard SonoPanel configuration for use by RMCC in a complete characterization to IEEE Standards. The results were reported under TTCP auspices. This is believed to be the first full scale matrix determination for 1-3 piezocomposites.

Stacked Composites:

SU and UDI have performed modelling work on stacked 1-3 composites, as well as some materials testing on diced devices. Under the TTCP, MSI made some stacked, unipolar piezocomposites having 30 volume % PZT in a hard polyurethane matrix, as well as two-layer devices having opposite polarity. Figures 43 and 44 show data from two-layer devices showing examples of both polarities, for which the impedance/frequency behavior were very similar and the thickness fundamental mode occurs at 90 kHz, as expected for a well-bonded composite. Figure 45 shows a modified multilayer composite in which the thickness mode resonance has been reduced to 45 kHz.

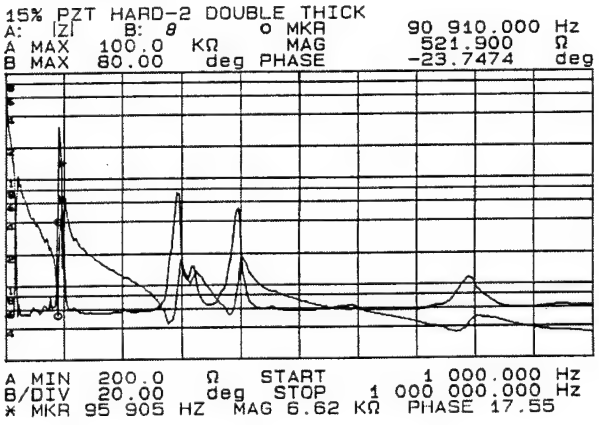

Figure 43. Impedance/frequency characteristics of unipolar double layer 1-3 piezocomposite in hard polyurethane matrix.

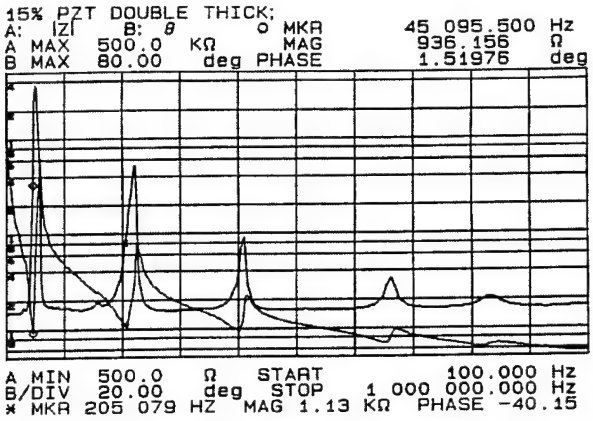

Figure 44. Impedance/frequency characteristics of multilayer 1-3 piezocomposite in hard polyurethane matrix.

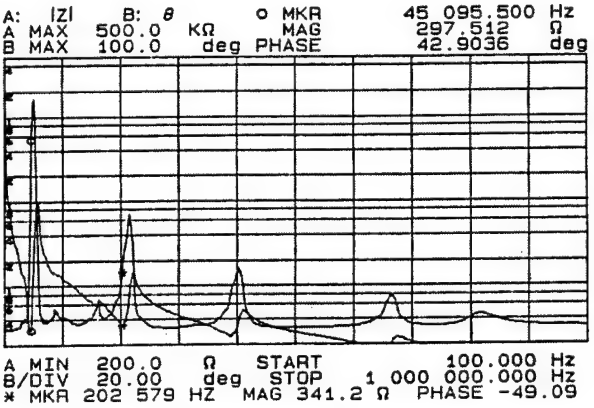

Figure 45. Impedance/frequency characteristics of modified 1-3 double layer piezocomposite in Shore D-85 polyurethane matrix.

Piezocomposites for Undersea Imaging:

A mine counter-measures (MCM) array development team was formed in 1994 for the purpose of developing advanced sonar array designs, and in particular, obtaining broad bandwidth, high sensitivity operation. Team tasks included identifying a practical MCM application which would benefit from advanced composite arrays, designing an array(s) to meet that application, simulating the design of these arrays using an advanced time-domain finite element code developed by WA, developing composite materials and array structures to improve array performance parameters, and building and testing feasibility of array structures and prototype arrays.

Following a review of potential undersea imaging applications, a particular forward-looking, slant beam application was selected. A trade study was conducted by TTCP members for system and array designs that would meet the system requirements for a minimum 90° scan sector and a minimum number of channels that would fit inside a 235 mm wide footprint. A curved array (Figure 46) solution was adopted over a phased array, since it places less stringent requirements on the element acceptance angle and required system delays. The goal array specifications are listed in Table 11.

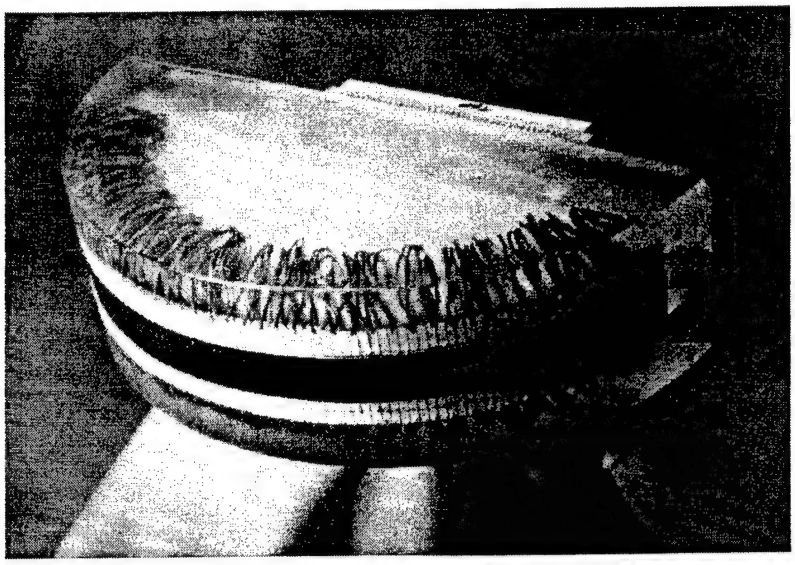

Figure 46. Photograph of 100 element prototype curved array.

Table11. Array requirements.

Center Frequency	375 kHZ
Bandwidth	250 kHz
Array Envelope	235 mm wide x 150 mm deep
Beamwidth	1.5° at 500 kHz
Vertical Beamwidth	15° at 500 kHz
Scan Sector with Full Beamwidth	90°

The requirement for 1.5° beams at 500 kHz yielded a 115 mm aperture. From grating lobe considerations, the pitch of the array was chosen to be one wavelength at the maximum frequency, or 3 mm at 500 kHz. Assuming that the maximum acceptance angle that can be obtained in an array of one wavelength pitch is ±30°, the minimum radius of a curved array with a 115 mm aperture was 115 mm from simple geometry. Achieving a 90° sector using a full 115 mm aperture over the entire sector required using a 150° curved array. The length of this array was 300 mm, which yielded 100 elements on a 3 mm pitch. The active length of the array is 120 mm, which yields 40 active elements for any one scan line. With this pitch, there were 60 scan lines in the 90° sector separated by 1.5°, matching the beamwidth parameter. The desired 15° vertical beamwidth at 500 kHz was obtained using an elevational aperture of 11.5 mm. The length of this 150°, 115 mm radius curved array projected onto the azimuthal axis was 232 mm, meeting the space requirement. A main issue with the use of this curved array was achieving the theoretical 30° acceptance angle in a composite array structure which could withstand some hydrostatic pressure.

TTCP team members at UDI-Fugro were also chartered to develop a system testbed for demonstrating this array. In the last year of the program, a non-real time digital beamformer was built that would not only switch between elements to slide the active aperture around the array, but also provide focusing for near-field imaging. This system

was used with the curved receiver array described, and a single element curved transmitter in imaging tests.

Composite and Array Design:

The piezoelectric material used in the array was a 1-3 composite of PZT ceramic in a polyurethane matrix. MSI's injection-molded composite technology, which was expected to lower the manufacturing cost of arrays, was chosen. The design of the composite was adjusted to fit MSI's capability in fine-scale composites. Several designs were considered based on some rules of thumb developed at the University of Strathclyde. Originally, it was desired to have at least 5 ceramic pillars in azimuth per element, and a 50% volume fraction ratio.

Several new composite configurations which were consistent MSI's molding technology at that time were designed, fabricated and tested under this task. They are shown schematically in Figure 47. The 2x8 configuration (Figure 47a) was investigated first because it could be fabricated from existing tooling. The 3x12 and 4x16 designs (Figures 47b and 47c) required considerable effort in new tooling designs and molding processes.

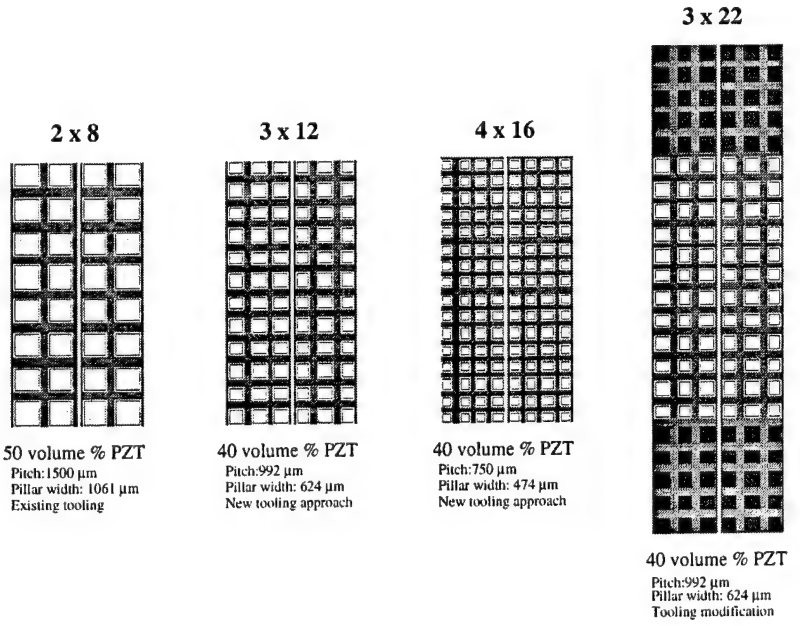

Figure 47. 1-3 composite designs investigated under the TTCP portion of this program.

Initial 3x12 molded preforms suffered from ejection problems, which led to broken pins. A variety of tooling modifications were implemented to solve this problem and produce good ceramic preforms (Figure 48). The most significant changes where the adjustment of the draft angle and careful polishing of the mold inserts. Similar development was performed with the 4x16 configurations with good results (Figure 47c). However, they were not ready at the time of the design down-selection, so 3x12 composite was used in array fabrication. The molding technology for this configuration is now mature and composite made from these preforms is being used in a variety of commercial applications.

The composite pillars in the 3x12 configuration were chosen to be 0.63 mm square and regularly spaced on a 1 mm pitch, leaving 3 pillars in azimuth and 12 pillars in elevation

under each element electrode. The element electrodes were separated by the 0.37 mm spacing between adjacent pillars as can be seen in Figure 47b.

Maximum sensitivity of a transducer is obtained by operating at resonance; many sonar devices have large bandwidths, obtained by operating below resonance, sacrificing sensitivity as a result. Following the usual practice in commercial applications, this array was designed to operate at resonance for maximum sensitivity and to use a matching layer to achieve up to one octave of bandwidth [8]. A single, continuous matching layer was designed to test the properties of the matching layer with the composite, and validate the effective composite parameters used in the simple 1D model. It was expected that good transducer characteristics would be obtained, including smooth bandshape response and the required bandwidth using a matching layer of 4.24 MRayl. This was demonstrated in an early prototype module.

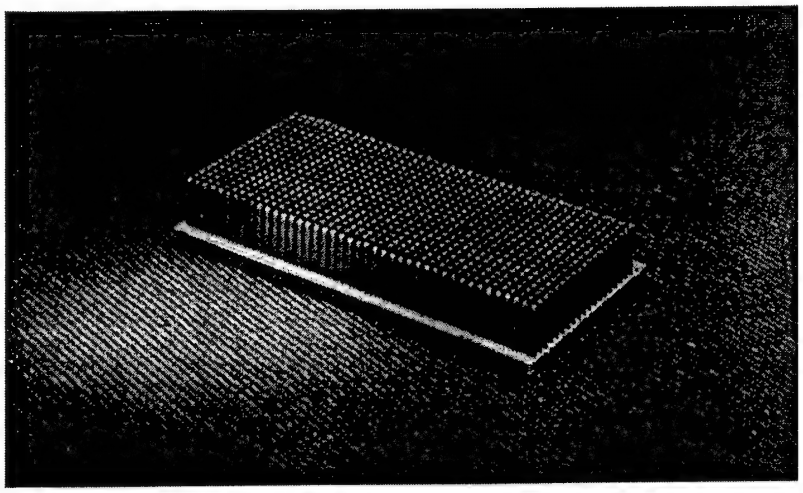

Figure 48. Photograph of a 3 x 12 PZT preform used in the prototype arrays.

Experience has shown that a continuous matching layer will limit the directivity pattern below the theoretical value, ±30° in this case. As expected, very low acceptance was observed on the array module with continuous matching layer. Therefore, a diced matching layer design was generated to solve this issue based on experience with medical arrays. Dicing the matching layer, however, increased the complexity of the design substantially, since a kerf filling material had to be found that not only keeps the elements decoupled to obtain the desired acceptance angle, but survive in a high pressure environment. In addition, the modes excited in the matching layer are considerably more complex since lateral modes in the diced matching layer will strongly couple to the preferred mode. Using simple coupled mode theory, which was shown to have good correlation to the lowest order symmetric Lamb wave [9], an effective velocity and impedance was generated to use in the design simulation tools. The matching layer structure was thoroughly simulated using the PZFlex FEM tool and compared to experimental results [10]. Within the range of matching layer aspect ratios considered, the FEM simulation showed that the effective velocity of the layer was identical to the asymptotic value obtained from coupled mode and Lamb wave theory over the large range of aspect ratios. This was a somewhat surprising result and warrants further study. The matching layer used was 1.8 mm thick and was diced completely through to the composite on a 3 mm pitch corresponding to the major element pitch, as can be seen in Figure 49.

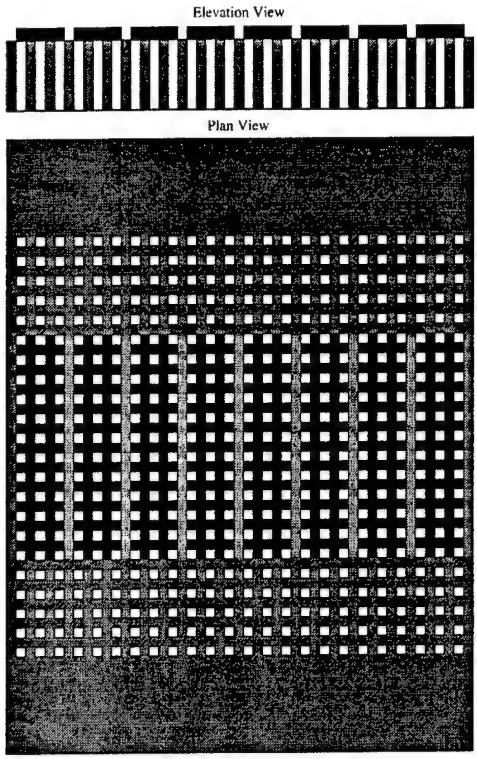

Figure 49. Schematic of the final array geometry without elevation apodization showing the 12 electroded elements.

Having generated the basic composite and matching layer design, the remaining key issues were the backing material, composite filler, and kerf filler materials. Since this array operated in receive mode only with long time delays between transmit and receive, almost any mechanically rigid backing would suffice. A simple low acoustic impedance mix of SD80 polyurethane and microballoons was used. The kerf filler was an entirely different story. Difficulties in measuring good properties of lossy polymers precluded using a simulation approach to this problem; consequently, many sample modules were constructed with various lossy composite filler and kerf filler materials in a totally empirical approach. These are described in the next section.

Array Construction and Test Results:

Several 7 element array modules (Figure 50) were built and tested using a relatively stiff Shore D80 polyurethane composite filler material. Several surprising results were obtained from these samples. While the composite by itself showed only very minor lateral and stopband resonances near the design passband, applying the matching layer caused many deleterious resonances to increase in strength and significantly reduce the usable bandwidth. In both the continuous and diced matching layer cases, a strong resonance at 350 kHz provided unacceptable passband ripple. In addition, the matching layer resonance was found to be considerably lower in frequency than predicted by the 1D model using effective velocities and impedances. This phenomenon can most easily be seen in Figure 51, which shows the electrical impedance of one element in a diced matching layer array module. Numerous and regularly spaced resonances are shown, in addition to coupled ceramic and matching layer resonances. Also, as expected, the acceptance angle was below $\pm 20^{\circ}$ for the continuous matching layer case. Unfortunately, the acceptance angle for the diced matching layer case showed little improvement.

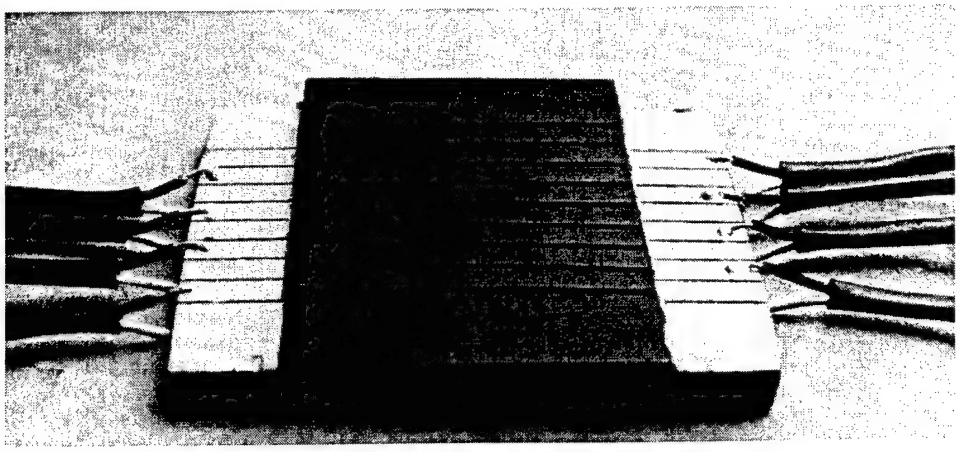

Figure 50. Photograph of one 7 element array module.

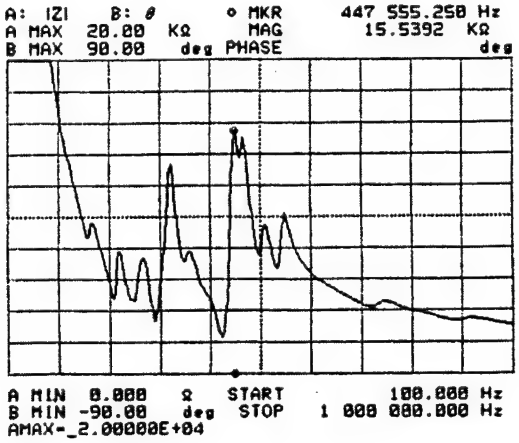

Figure 51. Air loaded electrical impedance magnitude of one test array element showing electronical harmonics.

After some consideration, it was agreed that these resonances were the result of lateral mode harmonics in the overall array module structure, most of which resulted from resonances in the 12 pillar, elevation direction. This became evident as the array manufacturing processes was steadily improved; the resonances were clearly regularly spaced harmonics of a low frequency fundamental, which corresponded roughly to the elevation dimension. These modes were also seen on a FEM generated impedance curve. It was concluded that a lossier composite filler material would need to be employed in order to damp out these resonances. Consequently, a series of samples were constructed using softer polyurethane fillers, including Shore D 70, Shore D 75, and Shore D 65, as well as some microballoon/urethane mixtures. Table 12 summarizes the construction of these coupons.

Table 12. Summary of the 7 element test coupons.

Coupon	Filler	Matching Layer	Encapsulation
1	Shore D 80	none	yes
2	Shore D 80	Shore D 80	yes
3	Shore D 80	epoxy	yes
4	Shore D 80	epoxy	no
5	Shore D 80	partially diced epoxy	no
6	Shore D 80	diced epoxy	no
7	Shore D 80	diced epoxy	no
8	voided (20%) Shore D 80	diced epoxy	no
9	Shore D 80	none	no
10	Shore D 75	diced epoxy	no
11	Shore D 65	diced epoxy	no
12	voided (20%) Shore D 75	diced epoxy	no
13	voided (20%) Shore D 65	diced epoxy	no
14	Shore D 65 (3x22)	diced epoxy	no
final	Shore D 65 (3x22)	diced epoxy	no

The microballoons had very little effect on dampening these resonances; softer fillers helped considerably, but not to the extent needed. Manufacturing concerns precluded using even softer materials than the gummy Shore D 65 urethane. At this point, the remaining avenue left was to increase the number of pillars in the elevation direction, still leaving only 12 electroded and electrically active. This lowered the fundamental elevational acoustic resonance and allowed a greater damping length to come into play for the harmful elevational harmonics. It was easy from a manufacturing standpoint to generate 22 pillars in elevation (see Figure 47); consequently, a final module was built in this configuration using the Shore D 65 filler material. The air-loaded electrical impedance of one element of this module (#14) is shown in Figure 52. These curves show little evidence of deleterious elevational harmonics and promised acceptable array performance parameters.

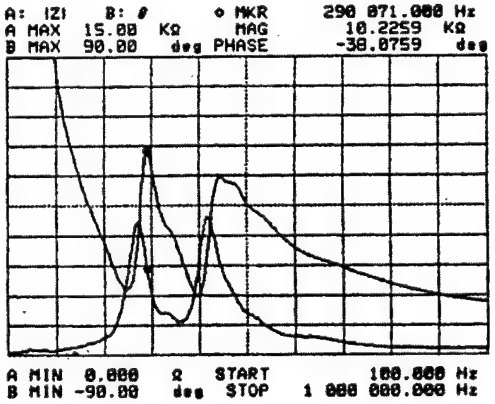

Figure 52. Air-loaded electrical impedance of array module #14 showing little evidence of electrical harmonics.

Two-way impulse and frequency response characteristics were generated for this array module with sealed air kerfs (Figure 53). The bandwidth is a less than the original

specification (320-425 kHz), but is still impressive for a resonant sonar array. The two-way acceptance angle is ±32° which is practically the theoretical limit.

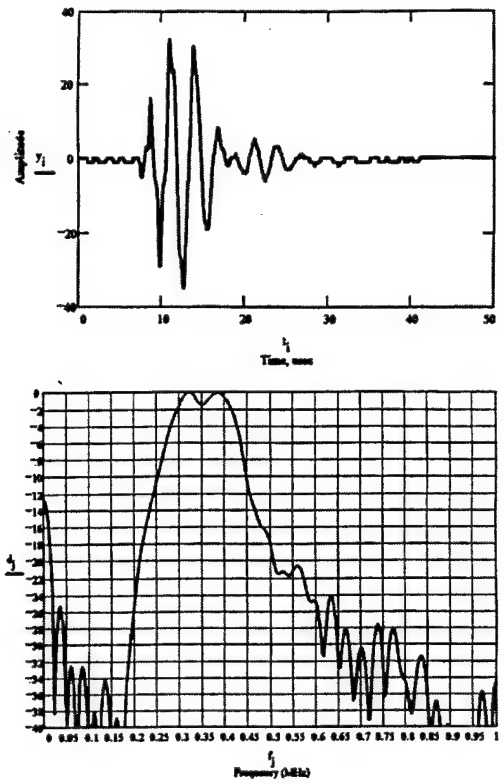

Figure 53. Time and frequency response of element of module #14 with air-filled kerfs.

However, sealed air gaps are unacceptable for a sonar array due to the high pressure undersea environment. This array module (#14) was kerf-filled with a standard sonar encapsulant urethane and retested. The bandwidth improved to 275-485 kHz (Figure 54), but the acceptance angle fell to only ±22° (Figure 55). This configuration was used in building the first two full 100 element curved arrays, while further modules were built to test additional kerf filler materials. No substantial improvement in the acceptance angle was noted using a variety of soft, lossy materials. Clearly the need for accurate material parameters for lossy polymers is needed as well in order to simulate this important parameter in FEM calculations. The final prototype (S/N 003) was therefore built with the same kerf filler as the previous two.

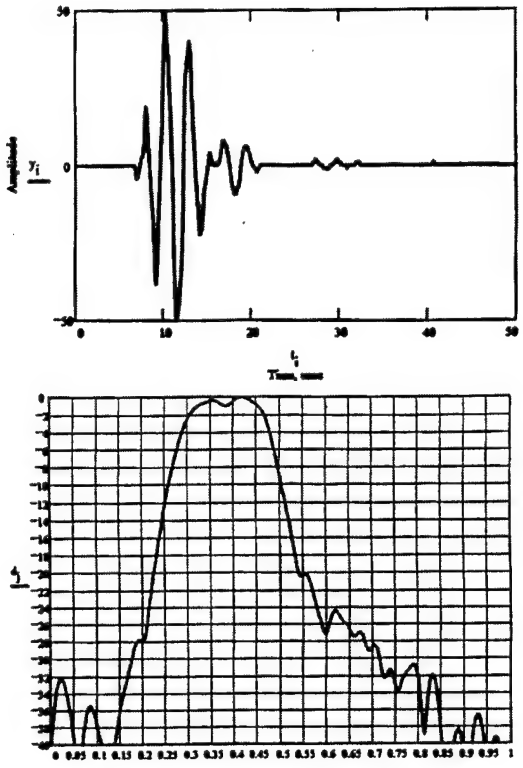

Figure 54. Time and frequency response of an element of module #14 with encapsulant-filled kerfs.

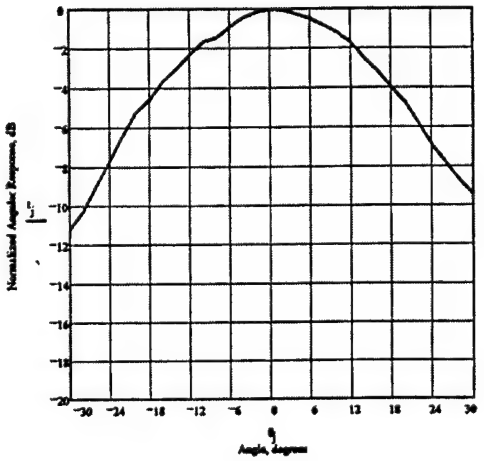

Figure 55. Broadband round trip angular response of an element of module #14 with filled kerfs.

After testing the final array test coupon, two 100 element prototype array were fabricated (Figure 46). Figure 57 shows the process flow for array fabrication. Ceramic preforms were molded, burned out, and sintered in 22 x 45 pin coupons with standard MSI injection molding techniques. These were filled with SD 65 polyurethane and then lapped to final thickness (Figure 57). The outer 10 elements were covered with a nonconductive urethane and then coated with a conductive silver epoxy which served as the electrode. The nonconductive urethane prevented the outer elements from being electrically addressed. A

filled epoxy matching layer was cast on each coupon and then diced through to the composite to separate both the matching layer and the individual array elements (Figure 58). A series of array modules were bonded together to form the full 100 element array, wires were attached, and the array curved to the desired shape. A circuit board which fans out from a standard connector to the array elements was bonded to the top and bottom of the curved composite (Figure 59). The circuit boards acted as both and electrical connection and a cavity for casting the voided urethane backing. Wires were soldered to the circuit board, and the entire array was cast in urethane. The urethane acted as both an encapsulant and a kerf filler.

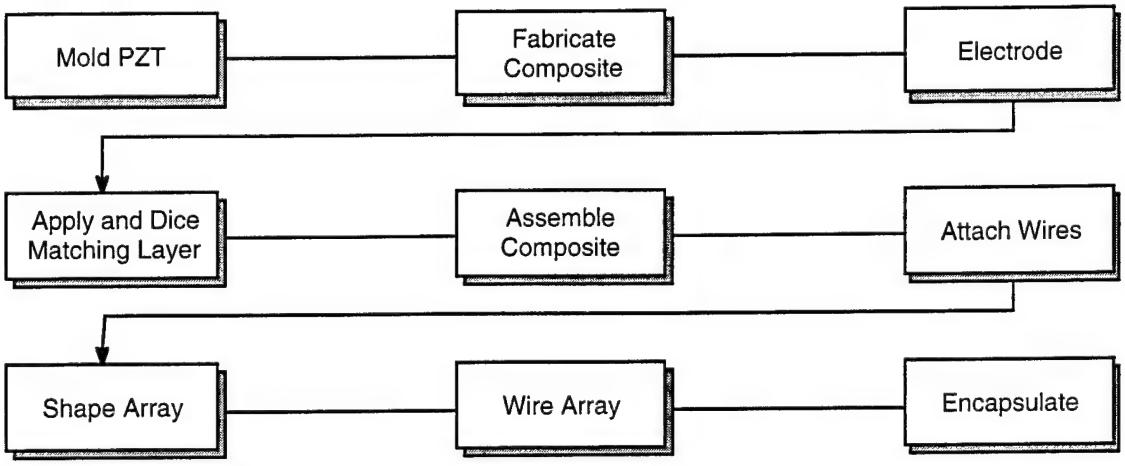

Figure 56. The process flow for fabricating the 100 element receive arrays.

Two full curved array prototypes were constructed by the method shown in Figure 57 with 100 active elements and sealed for undersea use. The first unit (S/N 001) was built for USRD, but was never shipped because of facility closings. The second prototype (S/N 002) was shipped to UDI-Fugro for calibrated array receive sensitivity and directivity tests, and incorporation into their demonstration imaging system. This particular array was slightly off radius on each end, which led to phase errors in the beamforming process away from the middle half of the array. A third array (S/N 003) was constructed which corrected this problem, and was also elevation apodized to reduce side lobes. A 16 x 3 apodization configuration as shown in Figure 60 was chosen. This was achieved by electroding the middle 3 x 10 pillars in elevation and extending the electrode pattern 1 x 3 additional pillars on both ends. Simulation of this pattern showed that the sidelobes should be reduced from -12 to -20 dB while maintaining the 15° beamwidth (at 500 kHz). This array had not been system tested as of this report date.

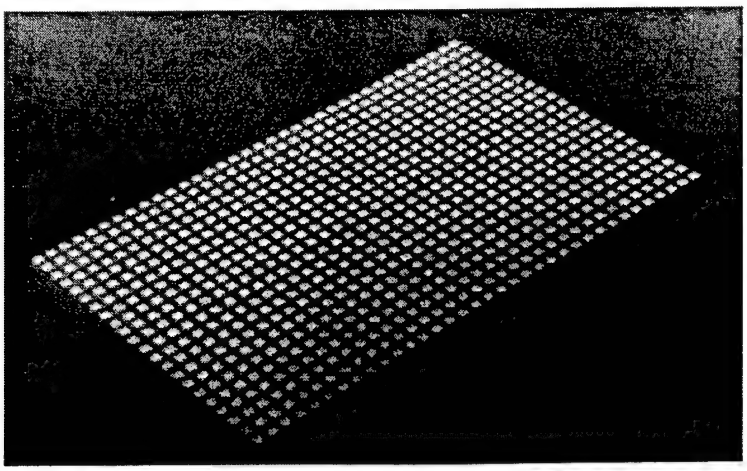

Figure 57. Photograph of one array module after lapping to final thickness.

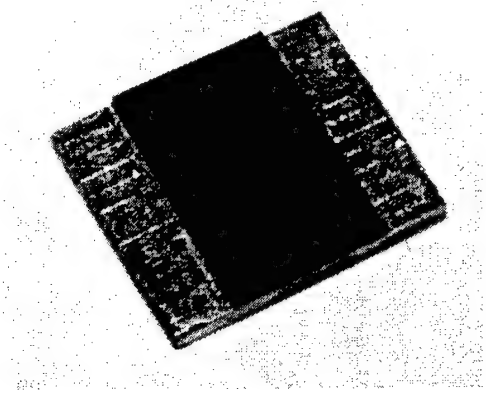

Figure 58. Photograph of an array module with diced matching layer.

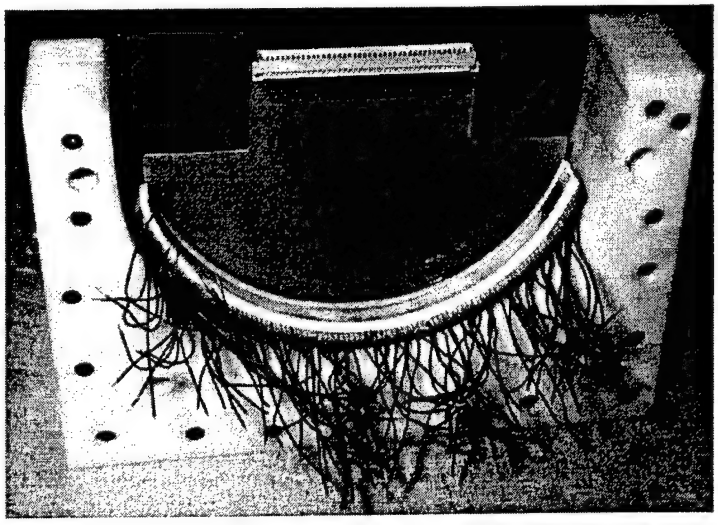

Figure 59. Photograph of a partially assembled curved array showing the integral circuit board.

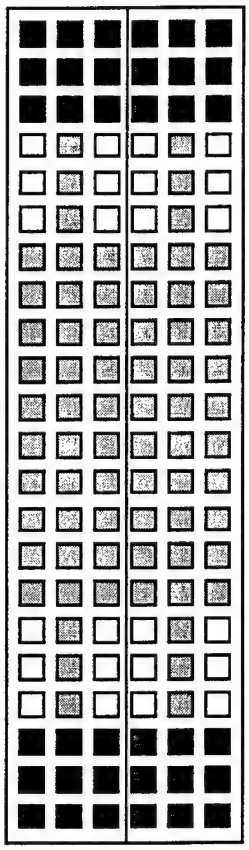

Figure 60. Schematic representation of two array elements showing the apodization pattern.

Capacitance and impedance measurements were measured for each element of every array before shipping. Figure 61 shows a typical impedance plot and Table 13 summarizes the capacitance results.

Table 13. Element capacitance results for the three prototype arrays.

	Average Capacitance ± σ
S/N 001	104.8 ± 9.6 (9.1%)
S/N 002	102.8 ± 7.2 (6.9%)
S/N 003	114.3 ± 10 (8.7%)

In addition to the capacitance and impedance measurements, UDI fully characterized array S/N 002. Theses results are summarized in Table 14.

Table 14. Array test results for S/N 002.

Max Receiver Sensitivity	-193 dB re 1V/μPa
-3 dB Bandwidth	208-453 kHz (74%)
Beamwidth, 250 kHz	± 31°
Beamwidth, 375 kHz	± 30.5°
Beamwidth, 500 kHz	± 24°

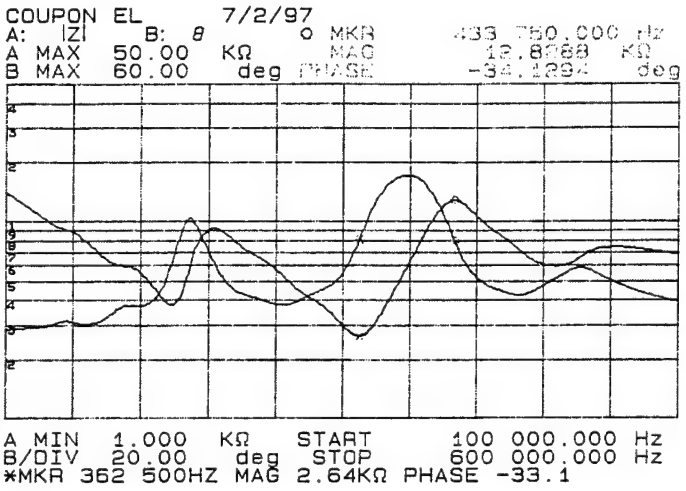

Figure 61. Typical impedance plot of one array element.

The sensitivity of this array was comparable to narrowband arrays currently in use, but its 74% bandwidth will allow for several broadband imaging modes to be employed. The element beamwidth was acceptable for most of the passband, falling off to 24° at 500 kHz. The second array with improved mechanical phase uniformity should prove useful in demonstrating broadband imaging modalities.

Other Applications Demonstrations

CAVES Sensors

Based on technical discussions among MSI, NRL, and NUWC (M. Moffett), an effort was undertaken to develop velocity sensors for potential use in the program. The motivation was to exploit MSI's low cost injection molding technology to manufacture the sensors for this application.

Traditionally, hydrophones (pressure sensors) have been used to detect underwater acoustic waves. Hydrophones have maximum sensitivity when mounted on a rigid backing surface. However, velocity sensors are more effective acoustic wave detectors for mounting on the compressible, pressure-release material now being used to coat the hulls of Navy vessels.

Velocity sensors should have the following characteristics:

- high sensitivity to motions normal to the mounting surface
- low transverse motion sensitivity
- low pressure (hydrophone) sensitivity
- low profile (thickness)
- area-averaged output
- low electronic noise floor (less than sea state 0 ambient acoustic noise)
- density equal to the pressure release materials (≈1.3 g/cc)
- stable to typical submarine hydrostatic pressures
- low cost

Most of the above requirements were demonstrated in this effort. Analytical and modeling support was provided by NRL (R. Corsaro).

Several 100 x 100 x 18 mm (4 x 4 x 0.7 inch) panels were produced. Each contained 16 net-shape molded monolithic PZT accelerometer elements (Figures 62 and 63) and a low noise pre-amplifier (Figure 64) in a neutrally-buoyant and water proof package (Figure 65). The low noise pre-amp was designed and fabricated by NRL.

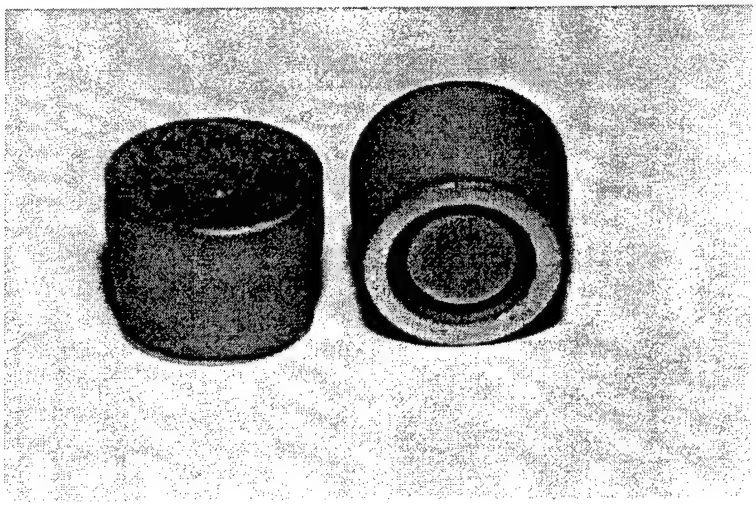

Figure 62. Net-shape molded PZT monolithic accelerometer elements used in the first generation CAVES panels.

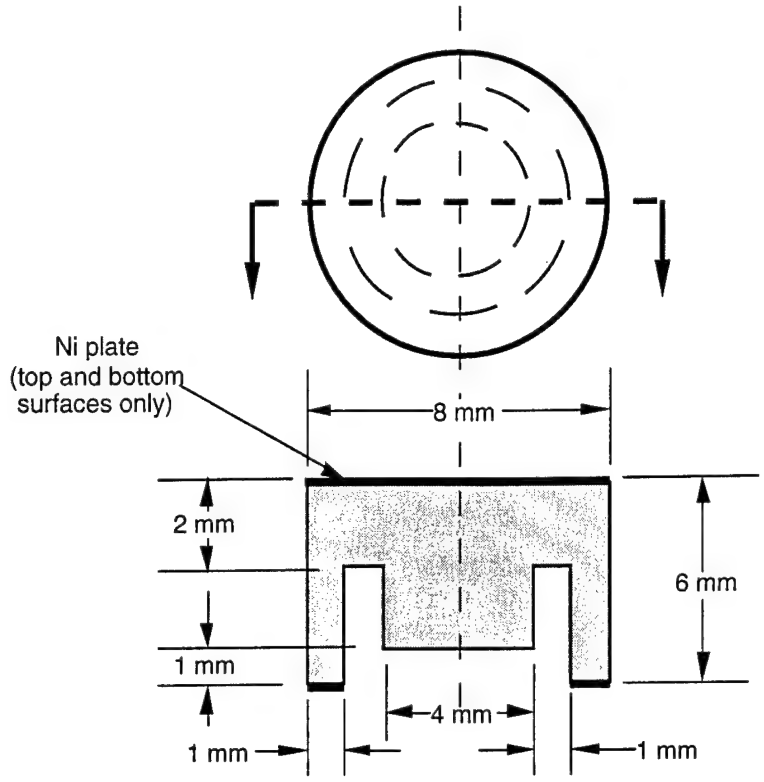

Figure 63. Drawing of monolithic PZT accelerometer elements used in the first generation panels.

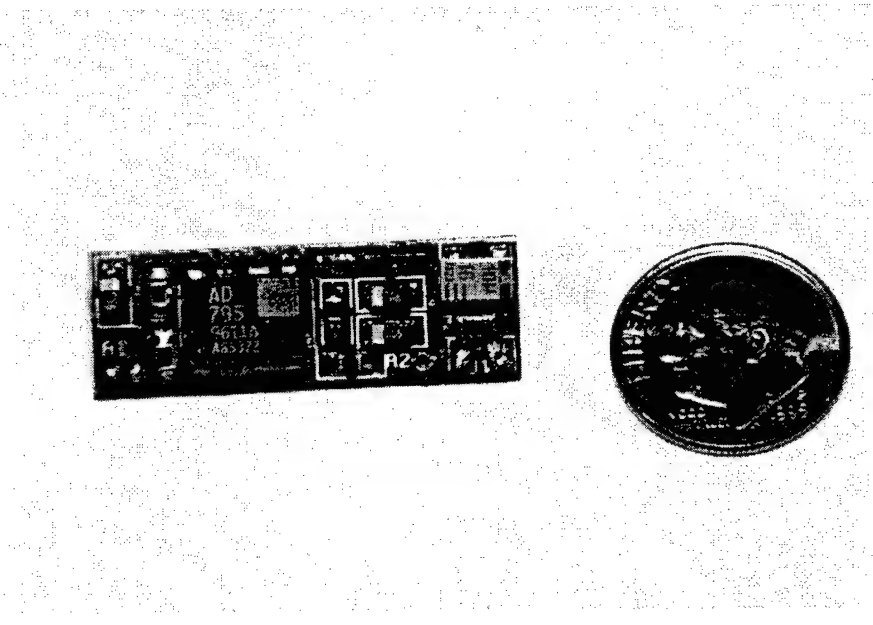

Figure 64. Low-noise pre-amplifier designed and fabricated by NRL and used on board the first generation accelerometer panels. The pre-amp dimensions are 10.7 x 32.7 x 6.3 mm.

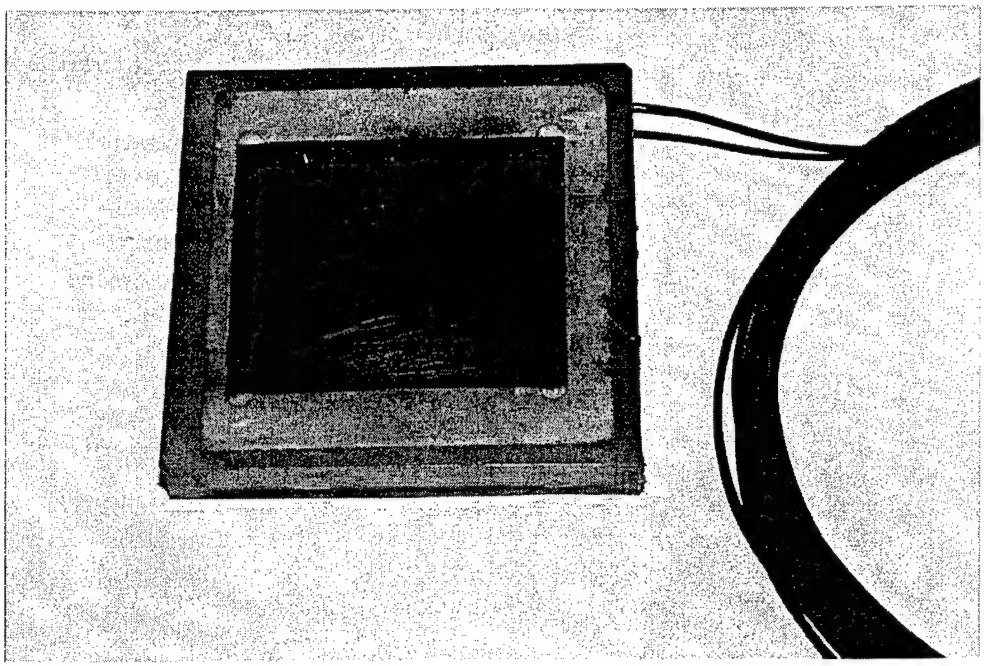

Figure 65. First generation accelerometer panels assembled by MSI and tested at NUWC-USRD. The panel measured 100 x 100 x 18 mm and contained 16 PZT monolithic accelerometer elements for area averaging.

Each accelerometer panel contained multiple net-shape formed monolithic PZT-5H accelerometer elements distributed throughout the panel in order to obtain an area-averaged response. The measured sensitivity of each accelerometer element was approximately 50 mV/g, in close agreement with prediction.

An important feature of the monolithic accelerometer device was that the mass and sensor elements were formed together from the same material and in the same manufacturing process. Separate construction of the mass was eliminated, as was the process of bonding the mass to the sensor. Reliability was improved since the bond uncertainty was not an issue in this monolithic design.

An accelerometer array, consisting of 16 monolithic PZT elements bonded to a GRP (glass reinforced polymer) board and used for the first generation panels, is shown in Figure 66.

The electrical signals from the multiple elements were combined and fed into an on-board pre-amplifier which drives a length of coaxial cable. For the first generation panels, a custom designed, low noise pre-amp was fabricated by NRL (Figure 64). Key specifications for the pre-amp are listed in Table 15.

Table 15. Pre-amp Specifications.

Gain	12 dB at 1.5 kHz
Supply voltage	18 VDC
Band width (±1 dB)	0.4 - 6.0 kHz
Noise	11 $nV/Hz^{1/2}$ at 1.5 kHz ; 0.6 $fA/Hz^{1/2}$
Dimensions	10.7 x 32.7 x 6.3 mm (0.42 x 1.29 x 0.25 inches)

MSI designed and implemented a low profile, low density package for the accelerometer panels. Rigid, low density (0.4 g/cc) syntactic foam was machined with chambers for the PZT elements and on-board pre-amp and recesses for the GRP board as well as the top and bottom steel plates. The machined syntactic foam configuration is shown in Figure 67. The GRP board and steel plates are bonded to the foam core with high strength epoxy. Figure 68 shows a partially assembled panel. The assembled package was then waterproofed with polyurethane (Figure 65).

The first generation panels showed good acceleration sensitivity when tested in air on a shaker table. The initial in-water evaluation of these first panels at the Naval Undersea Warfare Center - Underwater Sound Reference Detachment (NUWC-USRD) indicated a significant pressure sensitivity that is believed to be due to a base strain transmitted to the PZT element from the circuit board onto which it is mounted. This problem was further analyzed and solved under the new SmartPanels program (ONR/DARPA contract N00014-97-C-0236).

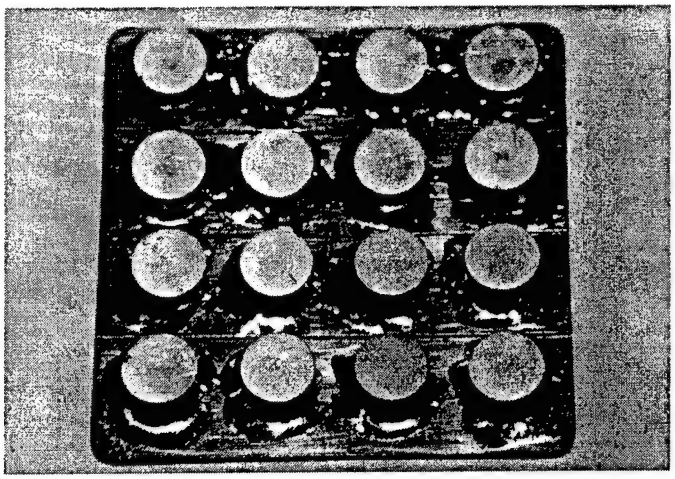

Figure 66. Photograph of 16 element PZT accelerometer array, with the individual elements soldered to a GRP board.

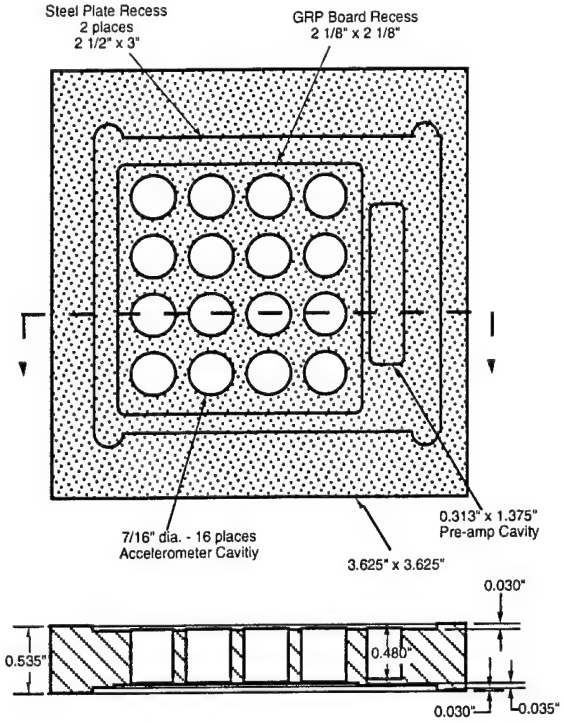

Figure 67. Configuration and dimensions of the rigid syntactic foam core used for the first generation accelerometer panels.

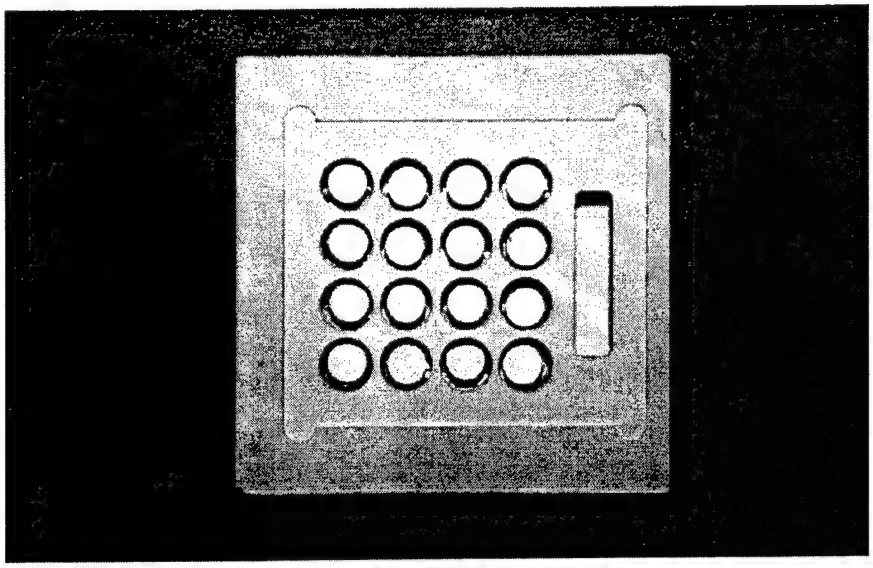

Figure 68. Partially assembled first generation accelerometer panel, showing pre-machined syntactic foam core with the 16 PZT accelerometer elements in place.

Hydrophone Arrays

The hydrophone array design in Track 4 was based on previous work to develop 1-3 composite arrays for submarine mine detection applications NUWC contract N66604-96-C-E978). The overall array dimensions were 7.608" x 3.998" x 0.300" with 0.705" x 0.953" individual elements. The composite material utilized PZT-5H ceramic in a "soft" (shore A60) polyurethane matrix. The ceramic component comprised 15% of the composite volume. Stiff, lightweight copper clad GRP coverplates were bonded to the composite surfaces to make the electrical connections to the ceramic elements. The coverplates were subsequently mechanically sectioned to define the individual elements in the array (Figure 69).

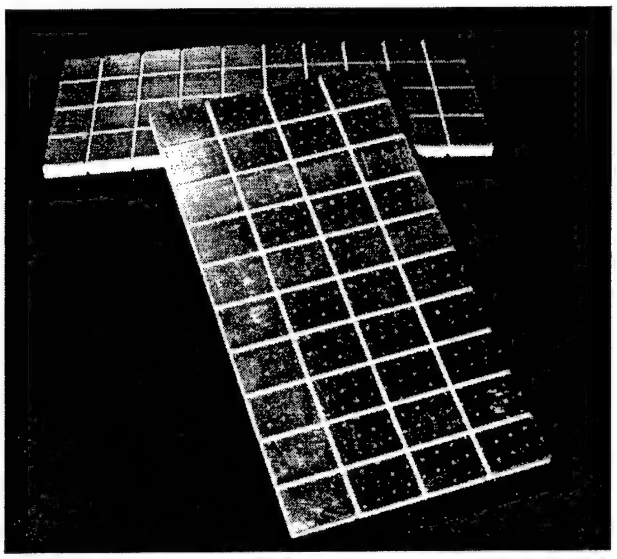

Figure 69. Photograph of top sectioned composite used to make the 40 element arrays.

The piezoelectric constant (d_{33}), capacitance, dielectric loss, and pressure sensitivity of each element in the finished array was measured. These are shown in Figures 70 and 71 and tabulated in Tables 16 and 17. Thirty feet of insulated electrical cable (type RG174) was attached to one side of each element, and a uniform ground plane was made by electrically connecting the other side of each element together. Two ground wires were run from the ground plane for redundancy.

One array (#103-1) was encapsulated in a waterproof polyurethane jacket. The other array (#103-2) was mounted onto a sound absorbing backing material (Syntech SADM-1) with a hole pattern that allowed the wiring to pass through it. The array and backing structure were then encapsulated in polyurethane waterproofing. Figure 72 is a photograph of the finished array (#103-2).

The finished arrays were delivered to NUWC, Newport, RI and subsequently shipped to Northrop-Grumman Ocean Systems, Annapolis, MD for testing.

Table 16. Characteristics of Array #103-1.

	Row 1	Row 2	Row 3	Row 4	Row 5	Row 6	Row 7	Row 8	Row 9	Row 10	
d33 (+)	550	600	540	540	565	565	540	590	590	575	
Cap. (pF)	399	380	384	407	392	406	415	389	400	399	Column
Loss	0.031	0.034	0.031	0.036	0.04	0.043	0.06	0.065	0.041	0.044	1
dBv (corr.)	-188.6	-188.4	-188.8	-188.5	-188.1	-188.9	-188.9	-188.8	-188.6	-188.0	
d33 (+)	565	590	585	540	545	530	555	550	550	575	
Cap. (pF)	389	424	399	392	420	439	407	408	400	409	Column
Loss	0.031	0.037	0.045	0.03	0.037	0.024	0.031	0.024	0.034	0.026	2
dBv (corr.)	-188.0	-188.5	-188.5	-188.2	-188.6	-188.6	-188.3	-189.1	-188.6	-187.9	
d33 (+)	630	555	555	540	540	520	550	525	555	585	
Cap. (pF)	384	406	424	409	431	445	399	418	421	422	Column
Loss	0.024	0.032	0.038	0.026	0.034	0.025	0.017	0.025	0.022	0.030	3
dBv (corr.)	-188.6	-188.8	-189.1	-188.6	-188.6	-188.6	-188.5	-188.6	-188.7	-188.5	
d33 (+)	625	560	575	565	590	580	560	570	580	650	
Cap. (pF)	383	388	394	398	397	407	414	409	417	420	Column
Loss	0.041	0.028	0.029	0.024	0.034	0.035	0.03	0.033	0.034	0.030	4
dBv (corr.)	-188.9	-188.8	-189.2	-188.9	-188.8	-188.9	-188.8	-189.1	-188.6	-188.4	

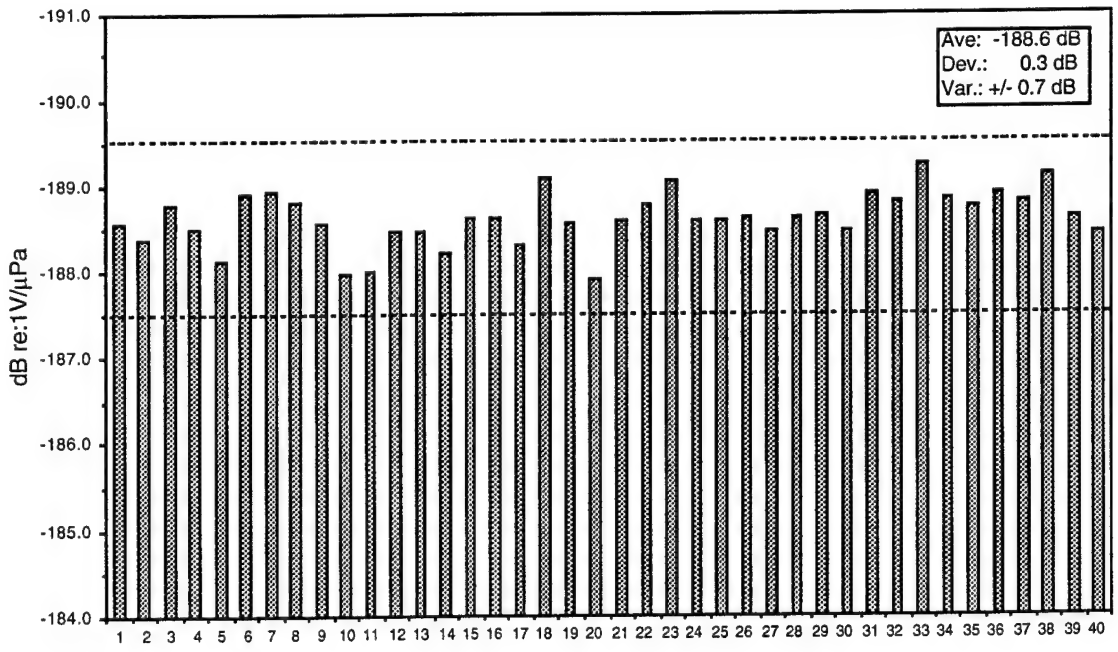

Figure 70. Graph showing the pressure sensitivity of array #103-1. Element to element uniformity is better than ±1dB.

Table 17. Characteristics of array #103-2.

	Row 1	Row 2	Row 3	Row 4	Row 5	Row 6	Row 7	Row 8	Row 9	Row 10	
d33 (+)	540	545	540	545	550	575	560	550	545	585	
Cap. (pF)	402	384	384	408	395	407	417	394	401	408	**Column**
Loss	0.028	0.027	0.030	0.038	0.035	0.033	0.048	0.061	0.046	0.037	**1**
dBv	-188.6	-187.7	-188.6	-188.4	-187.9	-188.8	-188.8	-188.6	-188.7	-188.7	
d33 (+)	530	580	570	550	550	570	540	530	535	570	
Cap. (pF)	389	422	402	402	430	433	403	407	403	407	**Column**
Loss	0.033	0.039	0.045	0.034	0.033	0.025	0.037	0.028	0.035	0.022	**2**
dBv	-187.9	-188.6	-188.1	-188.2	-188.5	-188.8	-188.5	-188.5	-188.3	-188.4	
d33 (+)	560	570	560	560	575	570	560	540	530	560	
Cap. (pF)	383	404	422	407	435	443	394	420	417	421	**Column**
Loss	0.029	0.038	0.026	0.026	0.031	0.032	0.026	0.027	0.024	0.031	**3**
dBv	-188.3	-188.4	-188.6	-188.5	-188.6	-188.6	-188.0	-188.6	-188.5	-188.4	
d33 (+)	555	535	530	560	545	550	525	520	525	560	
Cap. (pF)	389	384	388	400	385	405	408	408	411	417	**Column**
Loss	0.03	0.029	0.026	0.027	0.035	0.037	0.028	0.028	0.038	0.026	**4**
dBv	-188.6	-188.4	-188.5	-189.0	-188.4	-188.3	-188.5	-188.4	-188.5	-188.3	

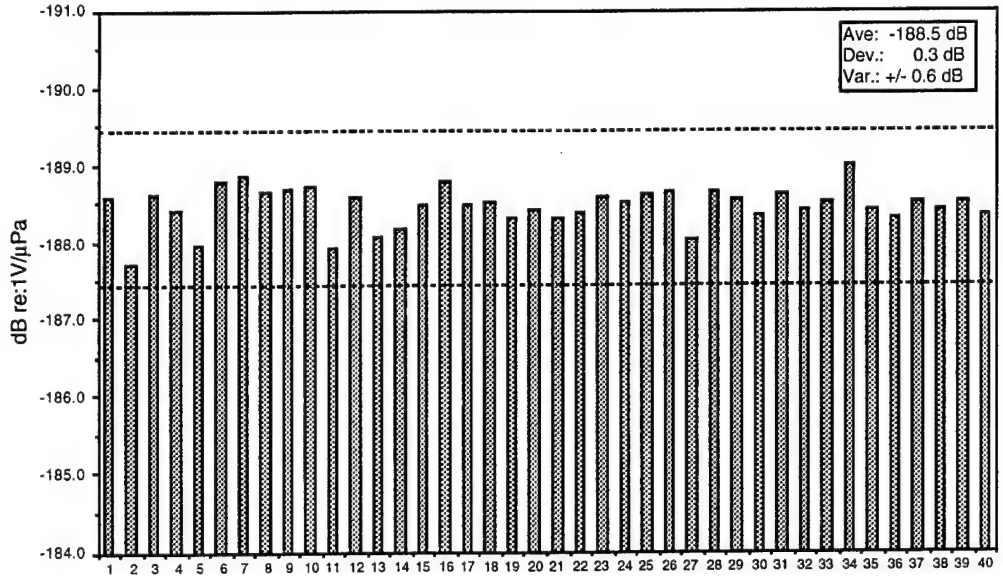

Figure 71. Graph showing the pressure sensitivity of array #103-2. Element to element uniformity is better than ±1dB.

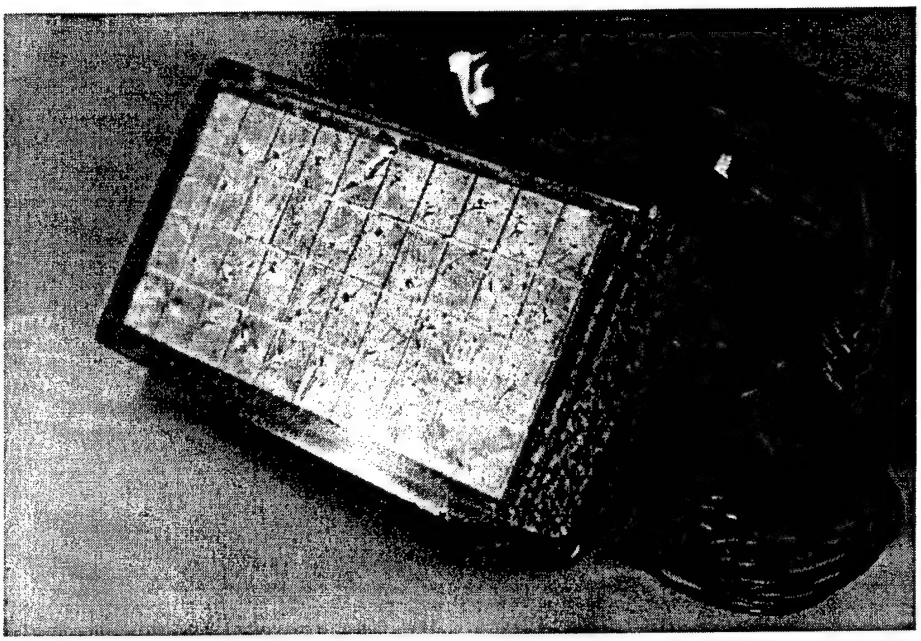

Figure 72. Photograph of the completed 40 element hydrophone array (#103-2).

4. Conclusions

Overall, the key program goals were met on schedule and within budget. The program impact was extended beyond fine scale 1-3 and 2-2 piezoceramic molding to include piezocomposite materials evaluation and transducer fabrication demonstrations. The program accomplishments included:

- New net-shaped forming technologies for producing fine scale 1-3 and 2-2 piezocomposite were developed.
- MSI demonstrated, for the first time, that ultrafine scale composites could be net-shape fabricated in reusable tooling.
- The 1-3 tooling approach was shown to be capable of molding dimensions down to 50 μm. The 2-2 tooling was used to demonstrate parts with dimensions down to at least 20 μm.
- The ultimate 1-3 piezocomposite dimensions achieved were 50 μm PZT rods at 0.25 PZT volume fraction.
- 2-2 composite with pitches of 45 μm and feature sizes less than 25 μm were finished and tested.
- Process and tooling refinement was performed to achieve larger area 1-3 composites, up to 30 mm square, with 100-150 μm diameter rods at 25% PZT volume fraction.
- A side by side comparison of injection molded and dice and fill 2-2 composites was performed by Tetrad Corporation. The injection molded composite performed well in comparison with the dice and fill composite and had slightly lower k_{31} values and less distinct SBERs, which are advantageous for thickness mode transducers.
- In collaboration with Tetrad Corporation, a 128 element high frequency linear imaging array was constructed and tested using fine-scale injection molded 2-2 composite. The images made with the composite array demonstrated the excellent quality that was expected from an array with 85% fractional bandwidth.
- 1-3 composite with diamond and triangular shaped elements were fabricated and evaluated at Strathclyde University to help understand interelement mode suppression.
- Several new types of double layer 1-3 piezocomposites with thickness mode resonance frequencies below 100 kHz were developed, including some with resonances as low as 45 kHz.
- A new molding technology was developed and used to produce 40 volume percent PZT preforms for frequency applications in the range of 250 kHz to 1 MHz.
- Two prototype electronically beam steered arrays were fabricated and delivered to UDI for systems integration and test.
- Several 100 x 100 x 8 mm accelerometer panels with integral low noise pre-amplifiers were produced and tested by NUWC-Newport. These showed good acceleration sensitivity in air on a shaker table.

- Two 40 element hydrophone arrays were fabricated, tested in-house and delivered to NUWC-Newport for evaluation in shipboard mine hunting applications.

5. Future Work

The efforts begun on high volume fraction, high frequency 1-3 composites are being continued on a new program, "Advanced Piezomaterials for Transducer Applications" (contract number N00014-97-C-0323). The program objective is to enhance the transmit performance, actuation authority and processability of advanced 1-3 and 2-2 piezocomposite materials through improved net-shape forming technology and piezomaterials optimization. The program offers a combined approach for enhancing the performance of piezocomposite transducers through optimization of the composite layout, materials and fabrication process. The program includes tasks for the development of high volume fraction piezocomposites and for the development of high displacement piezoceramics.

The tooling for fabricating high volume fraction composites will be similar to the one developed under this program to fabricate 40 volume percent PZT preforms. Particular attention will be paid to tool surface preparation and ejection methods. Initial development will begin with tooling capable of molding preforms with 0.5 mm pitch and PZT volume fraction of approximately 50%.

Based on recent transmit data obtained for 1-3 piezocomposite transducers (NRL, PSU-ARL, and Northrop-Grumman), soft piezoceramics function better under high drive conditions when configured in 1-3 form than the solid ceramic itself. This implies that the high power actuation performance of 1-3 piezocomposites can be enhanced by using softer piezoceramics for the composite elements without a significant overheating penalty. Softer piezoceramics are also in demand for both commercial and defense medical ultrasound applications. This portion of the effort aims to adapt and improve the properties of the PZT-relaxor family of soft piezoelectric ceramics (such as PNN-PZT) for these applications, and then to demonstrate net-shape process fabrication. The goal will be to establish an enhanced piezoceramic for use in piezocomposite transmitters, actuators and smart panels, and then ready the selected material for Navy application. The approach will be to adapt the selected piezoceramic through doping, so that the highest possible piezoelectric coefficients can be obtained, without lowering the Curie temperature to the point where application becomes impractical.

6. References

1. L. Bowen and K. French, "Fabrication of Piezoelectric Ceramic/Polymer Composites by Injection Molding", Proc. Int. Symp. on App. of Ferroelectrics, pp. 160-163, 1993.

2. U. Bast, D. Cramer, and A. Wolff, "A New Technique for the Production of Piezoelectric Composites with 1-3 Connectivity", Proc. 7th CIMTEC-World Ceramics Congress, pp. 2005-2015.

3. T. Howarth, paper presented at the IEEE Oceans Meeting, Halifax, NS, October 1997.

4. G. Hayward, paper presented at the 1994 IEEE Ultrasonics Symposium, Cannes, France.

5. ANSI/IEEE Standard 176, 1987 IEEE Standard on Piezoelectricity, IEEE New York, NY 1978.

6. 61 IRE 14.S1, IRE Standards on Piezoelectric Crystals: Measurements of Piezoelectric Ceramics, 1961, IRE, New York, NY 1961.

7. C. G. Oakley, "Geometric Effects on the Stopband Structure of 2-2 Piezoelectric Composite Plates", IEEE Ultrasonics Symp. 1991.

8. C. S. Desilets, J. D. Fraser, and G. S. Kino, "The Design of Efficient Broad-Band Piezoelectric Transducers", IEEE Trans. on Sonics and Ultrasonics, **SU-25** pp. 115-125, 1978.

9. S. Ayter, "Transmission Line Modeling for Array Transducer Elements", Proc. of the 1990 IEEE Ultrasonics Symp., pp. 791-794, 1990.

10. G. Wojcik, C. Desilets, L. Nikodym, D. Vaughan, N. Abboud, and J. Mould, "Computer Modeling of Diced Matching Layers", Proc. of the 1996 IEEE Ultrasonics Symp., pp. 1503-1508, 1996.

7. Presentations and Papers Incorporating Program Data

1. Leslie J. Bowen, Richard L. Gentilman, Hong T. Pham, Daniel F. Fiore, and Kenneth W. French, "Injection Molded Fine-Scale Piezoelectric Composite Transducers", IEEE Ultrasonics Symposium Proceedings, pp. 449-503, 1993.

2. Leslie Bowen, Richard Gentilman, Daniel Fiore, Hong Pham, William Serwatka, Craig Near and Brian Pazol, "Design, Fabrication, and Properties of Sonopanel™ 1-3 Piezocomposite Transducers", Ferroelectrics **187**, 109 (1996).

3. Leslie J. Bowen, Brian G. Pazol, Hong T. Pham, William R. Serwatka, Daniel F. Fiore, Craig D. Near and Richard L. Gentilman, "Fabrication and Performance of Net-Shape Piezocomposite Transducers", US/Japan Ceramics Proceedings, November 1995.

4. B. G. Pazol, L. J. Bowen, R. L. Gentilman, H. T. Pham, W. J. Serwatka, C. G. Oakley, and D. R. Dietz, "Ultrafine Scale Piezoelectric Composite Materials for High Frequency Ultrasonic Imaging", IEEE Ultrasonics Symposium Proceedings, vol. 2, November 1995.

5. B. G. Pazol, L. J. Bowen, R. L. Gentilman, H. T. Pham-Nguyen, and W. J. Serwatka, "Ultrafine Scale Piezoelectric Composite Materials for High Frequency Applications", 1996 ONR Materials and Transducers Workshop, State College, PA, March 1996.

6. R. Gentilman, D. Fiore, H. Pham-Nguyen, W. Serwatka, C. Near, P. McGuire, and L. Bowen, "Recent Advances in Piezocomposite Materials, Transducers, and arrays at MSI", 1996 ONR Materials and Transducers Workshop, State College, PA, March 1996.

7. L. Bowen, C. Desilets, G. Hayward, C. Maclean, B. Mukherjee, V. Murray, L. Kikodym, B. Pazol, S. Sherrit, and G. Wojcik, "Composite Curved Linear Array

for Sonar Imaging: Construction, Testing, and Comparison to FEM Simulations", 1997 ONR Materials and Transducers Workshop, State College, PA, April 1997.

8. B. Pazol, J. Hollenbeck, R. Gentilman, H. Pham-Nguyen, G. Schmidt, and L. Bowen, "Advances in Large Scale Piezoelectric Composite Material Fabrication", 1997 ONR Materials and Transducers Workshop, State College, PA, April 1997.

9. R. Gentilman, D. Fiore, B. Pazol, C. Near, G. Schmidt, K. Markowski, P. McGuire, K. Gabriel, J. Glynn, and L. Bowen, "Recent Developments in 1-3 Piezocomposite Materials, Transducers, Arrays, and Smart Panels", 1997 ONR Materials and Transducers Workshop, State College, PA, April 1997.

10. C. Desilets, M. Callahan, G. Haywood, C. Maclean, B. Mukherjee, V. Murray, L. Nikodym, B. Pazol, S. Sherrit, G. Wojcik, "Composite Curved Linear Array for Sonar Imaging: Construction, Testing, and Comparison to FEM Simulations", IEEE International Symposium, October 1997.

11. B. Pazol, H. Pham-Nguyen, J. Hollenbeck, M. Callahan, K. Gabriel, and G. Schmidt, "Piezocomposite Materials for Ultrasonic Imaging Applications", Proceedings of the 8th US-Japan Seminar on Dielectric and Piezoelectric Ceramics, Plymouth, MA, October 1997.